DOI: 10.1002/ejoc.200600100

π-Prismands – Flexible Hosts for Metal Ions

Andreas Kunze,[b] Saeed Balalaie,[a,c] Rolf Gleiter,*[a] and Frank Rominger[a]

Keywords: Prismands / Cage compounds / Alkynes / Metal complexes

The π-prismands dealt with in this paper are: 1,8-diazabicyclo[6.6.6]eicosa-4,11,17-triyne (**6**), 1,8-diazabicyclo[6.6.5]-nonadeca-4,11-diyne (**7**), 1,8-diazabicyclo[6.6.6]eicosa-4,11-diyne (**8**), 1,10-diazabicyclo[8.6.6]docosa-5,13,19-triyne (**9**), 17-(1,4)benzena-1,8-diazabicyclo[6.6.5]nonadecaphane-4,11-diyne (**10**), 11,16-(1,4)dibenzena-1,8-diazabicyclo[6.5.5]octadecaphane-4-yne (**11**) and 4,10,15-(1,4)tribenzena-1,7-diazabicyclo[5.5.5]heptadecaphane (**12**). The synthesis of **9** is reported. The molecular parameters obtained from X-ray investigations on single crystals of **6**–**9** as well as of **10**–**12** are compared with each other. Also discussed are the structures of the monoprotonated forms of **6** and **12**. The π-prismands **6**–**12** form stable complexes with Ag^+ and Cu^+. The crystal structures of the metal complexes as well as their spectroscopic properties are reported. Both reveal that the metal center interacts with the nitrogen atoms and the π-systems of the bridges.

Introduction

1,(*k*+2)-diazabicyclo[*k.l.m*]alkanes (**1**) are of interest with respect to their stereochemistry and their properties.[1] The detailed investigation of these species by Alder et al.[2] revealed that those species with *k*, *l*, *m* ≥ 3–6 show an *in*/*in* conformation and act as proton sponges with the proton in the cage.[3a] In the monoprotonated form of 1,6-diazabicyclo[4.4.4]tetradecane (**2**·H)$^+$ a strong hydrogen bond between the two bridgehead nitrogen atoms has been reported.[3b] Systems with longer bridges, such as 1,8-diazabicyclo[6.6.6]eicosane, 1,8-diazabicyclo[6.6.5]nonadecane and 1,8-diazabicyclo[6.6.4]octadecane[4] show a kinetically controlled protonation reaction yielding mixtures of the *out*/*out* and *in*/*out* diprotonated species. The thermodynamically more stable species, the *in*/*in* conformers, were formed at higher temperatures and longer reaction times.[4] It is interesting to note that no metal complexes of those 1,(*k*+2)-diazabicyclo[*k.l.m*]alkanes are reported where all three bridges are pure hydrocarbon chains.[2] This situation changes when ether bridges are used between the nitrogen centers as in the [1.1.1]cryptand (**3**)[5] or 4,7-dioxa-1,10-diazabicyclo[8.6.6]docosa-13,19-diyne (**4**)[6a] and the corresponding dithia derivative **5**.[6b] For **4** complexes with lithium, sodium, cadmium, copper(I), and silver were isolated.[6a] For **5** copper(I) and silver complexes were characterized.[6b] We thought it of interest to replace one of the CH_2 groups in each chain of **1** by a π-donor, such as a triple bond or a cyclic conjugated π-system, anticipating that the resulting species in which three π-ligands are oriented along a C_3 axis, also called π-prismands,[7] could be capable of complexing metal ions.

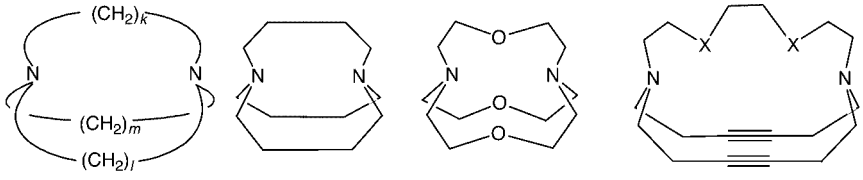

1 **2** **3** **4, 5**

The ligands and their metal complexes we report in this work are 1,8-diazabicyclo[6.6.6]eicosa-4,11,17-triyne (**6**),[8] 1,8-diazabicyclo[6.6.5]nona-deca-4,11-diyne (**7**),[8] 1,8-diazabicyclo[6.6.6]eicosa-4,11-diyne (**8**),[8] 1,10-diazabicyclo-[8.6.6]docosa-5,13,19-triyne (**9**), 17-(1,4)benzena-1,8-diaza-

[a] Organisch-Chemisches Institut der Universität Heidelberg, Im Neuenheimer Feld 270, 69120 Heidelberg, Germany
E-mail: rolf.gleiter@oci.uni-heidelberg.de
[b] Carbogen AG, Schachenallee 29, 5001 Aarau, Switzerland
[c] Department of Chemistry, K. N. Toosi University of Technology, Teheran, Iran

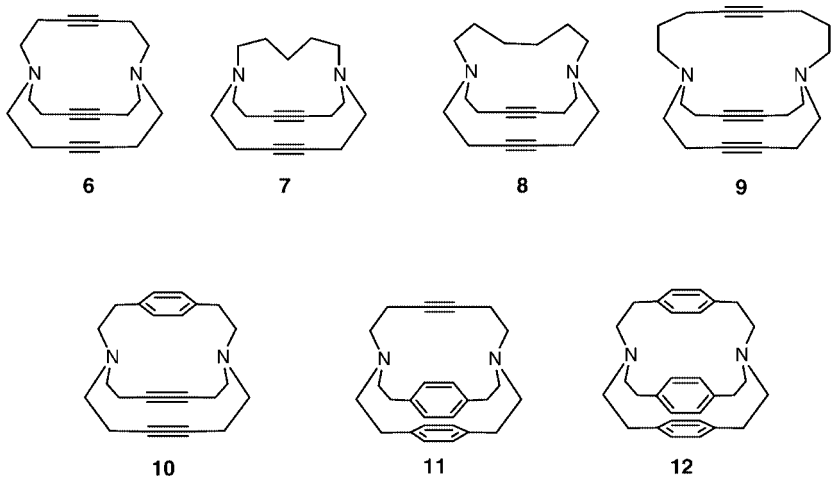

bicyclo[6.6.5]nonadecaphane-4,11-diyne (**10**),[9] 11,16-(1,4)-dibenzena-1,8-diazabicyclo[6.5.5]octodecaphane-4-yne (**11**)[9] and 4,10,15-(1,4)tribenzena-1,7-diazabicyclo[5.5.5]heptadecaphane (**12**).[9]

Results and Discussion

Syntheses and Properties of the Ligands

a) Syntheses

The syntheses of all six π-prismands were accomplished by a three-component condensation[8,9] of α,ω-dibromides with α,ω-diamines as shown in Scheme 1. The condensation was carried out in refluxing acetonitrile in the presence of potassium carbonate as a base and K^+ as template. The syntheses of **6**–**8**[8] and **10**–**12**[9] have been described briefly in the literature. The synthesis of **9** follows the protocol of Scheme 1. As starting material for **9** we used 1,6-dibromohex-3-yne (**13**)[10] and 1,8-diaminooct-4-yne (**14**)[11] yielding 29% of **9**.

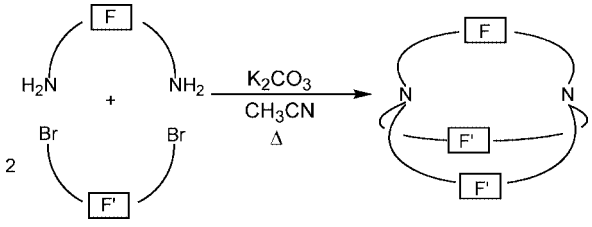

Scheme 1.

It is interesting to note that the highly symmetrical cryptands **6** and **12** are those with the highest melting points (212 °C and 192 °C, respectively) whereas the more flexible compounds **7** (85 °C), **8** (124 °C), **9** (156 °C), **10** (114 °C), and **11** (107 °C) melt at considerably lower temperatures.

b) Spectroscopic Investigations

The chemical shift of the ^{13}C signals for the sp-hybridized carbon atom in **6**–**11** varies only slightly from δ = 77.0 (**11**) to δ = 80.2 ppm (**9**). These values are close to that recorded for hex-3-yne (δ = 80.9 ppm) and indicative of no ring strain as found e.g. for cyclooctyne (δ = 94.4 ppm).[12] The ^1H NMR spectra of **10**–**12** measured at room temperature reveal that the chemical shifts of the aromatic protons of **10** (A A′ A′′ A′′′) and **11** (A A′ B B′) are located in the anticipated aromatic region, whereas those of **12** (A A′ A′′ A′′′) exhibit a rather high-field resonance. This was ascribed to a mutual transannular shielding due to a rotation process as discussed below. The UV data of **10**–**12** reveal a band between 266 nm (**10**) and 268 nm (**11**, **12**) indicating a planarity of the rings as in *p*-xylene (λ_{max} = 273 nm).[13]

To detect any dynamic processes of the cage skeleton we have recorded the ^1H and ^{13}C NMR spectra of **6**, **10**, **11**, and **12** at variable temperatures. For **6** the ^1H NMR spectrum taken at 20 °C shows two triplets at δ = 2.23 and 2.43 ppm with a coupling constant of ^3J = 5.2 Hz. At 178 K both signals coalesce, which allows an estimate of the free activation enthalpy $\Delta G^{\neq}$ of a dynamic process[14] [$\Delta\nu$ = 77 Hz, T_c = 178 K, $\Delta G_c^{\neq} \approx 8$ kcal/mol, $k(T_c) \approx 170\ s^{-1}$]. For this process we can envisage the rearrangement of one helical enantiomer (D_3) into the other as shown in Figure 1 (bottom). However, the transition state for such a process would be of D_{3h} symmetry with an ecliptic conformation of all six ethano bridges. A more favorable process should be a two-step mechanism in which the helical isomer arranges to a paddle-wheel (C_{3h}) conformation, which in turn rearranges to the enantiomeric form of D_3 symmetry (see Figure 1).

The dynamical processes of **11** and **12** have been reported in a preliminary publication.[9] Recently, we were also able to record the data for **10**. For all three species the temperature of coalescence (T_c), the frequency difference ($\Delta\nu$) and the estimated activation enthalpies[14] ($\Delta G^{\neq}$) are listed in Table 1. A comparison with values derived from an AM1 calculation[15] shows a good agreement for **11** and **12** if a

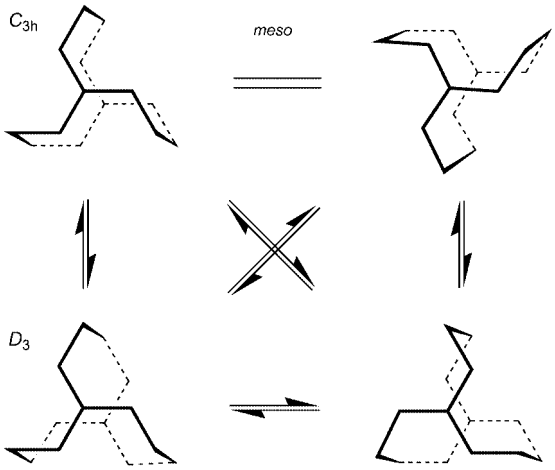

Figure 1. Schematic presentation of the dynamic processes causing a racemisation of **6** from one D_3 enantiomer to the other.

rotation of only one benzene ring is assumed. The higher $\Delta G^{\neq}$ value for **11** (15.6 kcal/mol) compared to that for **12** (9.3 kcal/mol) can be ascribed to the larger N···N distance in the latter case (6.145 Å) compared to that calculated for **11** (5.772 Å). For **10** we assume that the dynamic process is not caused by the rotation of the benzene ring but that an equilibration between the helical and paddle-wheel conformation is observed as discussed for **6** and outlined in Figure 1. Due to the small N···N distance in **10** (5.130 Å) the activation energy for the rotation of the benzene ring was calculated to be 25 kcal/mol (Table 1).

Table 1. Comparison between the measured and calculated free activation enthalpies [kcal/mol] for **10**–**12**. Also listed are the temperatures of coalescence (T_c) and the frequency difference ($\Delta\nu$).

Compd.	T_c [K]	$\Delta\nu$ [Hz]	$\Delta G^{\neq}_{c\ exp}$	Ar(rot)[a]	$\Delta G^{\neq}_{(AM1)}$
10	193	10	9.9	1	25.0
11	321	68	15.6	1	16.4
				2	52.3
				1	8.9
12	191	36	9.3	2	57.5
				3	103.9

[a] Number of rotating benzene rings.

c) Structural Investigations

X-ray structural investigations on single crystals of **6**,[8b] **7**[8a] and **12**[9] have been reported previously. In the mean time we were also able to record the structural parameters of **9** and **10**. Their molecular structures are shown in Figure 2. A comparison of selected distances obtained for these two species with those of **6** and **12** is listed in Table 2. For **11** the values were derived by DFT calculations,[16,17] varying all geometrical parameters. It can be seen that replacement of one 3-hexyne bridge in **6** by a 4-octyne bridge (**9**) only leads to a slight increase of the N···N distance from 5.05 Å (**6**) to 5.10 Å (**9**), whereas replacement of the triple bonds in **6** by benzene rings (**10**, **11**, **12**) increases the N···N distance by about 0.3 Å per benzene ring.

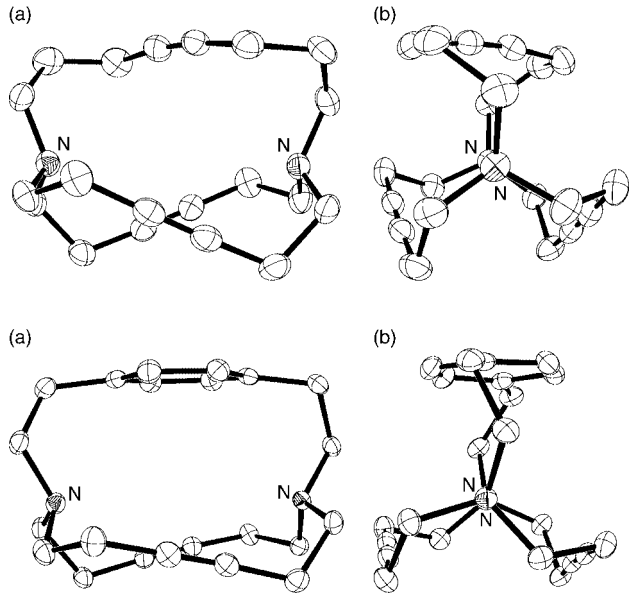

Figure 2. Molecular structures of **9** (top) and **10**; a) side view; b) view along the N···N axis. The hydrogen atoms and the anions are omitted for the sake of clarity.

Table 2. Comparison of selected distances [Å] and angles [°] of **6** and **9**–**12** in the solid state.

	6[8]	**9**	**10**	**11**[f]	**12**[9]
N···N	5.049(2)	5.103(2)	5.30(2)	(5.772)[f]	6.14(4)[e]
$\Sigma\omega_N$[a]	345.0(3)	337.2(3)	334.6(2)	(335.6)[f]	329.3(2)
π···π[b]	3.760(2)	3.791(3)	3.982(2)	–	–
		4.085(3)			
		3.996(3)			
π···π[c]	–	–	4.327(2)	(4.198)[f]	–
			4.268(2)		
π···π[d]	–	–	–	(4.714)[f]	4.51(5)

[a] Sum of the bond angles at the nitrogen atoms. [b] Transannular distances between the center of the triple bonds. [c] Transannular distances between triple bonds and aromatic ring. [d] Transannular distances between aromatic rings. [e] Average value. [f] Values derived by DFT calculations.

Protonation of 6 and 12

The protonation of **6** could be achieved with trifluoroacetic acid (TFAA) in $CDCl_3$, CD_3OD and D_2O. Depending on the amount of TFAA added, it was possible to obtain selectively $[\mathbf{6}\cdot H]^+$ and $[\mathbf{6}\cdot 2H]^{2+}$. In $CDCl_3$ 3 equiv. of acid were necessary to produce the monoprotonated form, whereas in methanol 1 equiv. was sufficient. In D_2O 3 equiv. of TFAA quantitatively produced the diprotonated system.[18]

To obtain more structural information on $[\mathbf{6}\cdot H]^+$ and $[\mathbf{6}\cdot 2H]^{2+}$, we tried to isolate single crystals. For $[\mathbf{6}\cdot H]^+$ we were successful when we treated **6** in ether with equimolar amounts of HBF_4. This yielded $[\mathbf{6}\cdot H]^+BF_4^-$. The dication $[\mathbf{6}\cdot 2H]^{2+}$ could be isolated with the triflate anion.[18] The N···N distances and the bond angles at the nitrogen atoms of **6**, $[\mathbf{6}\cdot H]^+$ and $[\mathbf{6}\cdot 2H]^{2+}$ are compared in Table 3. The monoprotonation reduces the distance between the nitrogen centers considerably. As a consequence, one observes a re-

duction of the bond angles at the nitrogen atoms. An attractive dipolar interaction between the NH bond and the lone pair at the opposite nitrogen center might increase the shrinking of the N···N distance. Furthermore, one observes with shrinking N···N distance an enlargement of the π···π distance (Table 3). These changes in distances in the series **6**, [**6**·H]$^+$ and [**6**·2H]$^{2+}$ go along with a change in conformation. This is demonstrated in Figure 4 (see below), where this series is expanded with the metal complexes. For the monoprotonated species [**6**·H]$^+$ no intramolecular proton transfer could be detected when heating a sample in 1,1,2,2-tetrachloro[D_2]ethane to 130 °C. In the ^{15}N NMR spectrum of [**6**·H]$^+$ we find the signal of the protonated nitrogen atom at δ = –301.3 ppm and that of the unprotonated nitrogen atom at δ = –314.0 ppm; in both cases we find a low-field shift as compared to **6** (δ = –318.0 ppm). Furthermore, it is noteworthy that the ^{13}C NMR spectroscopic data of the alkyne unit in [**6**·H]$^+$ (δ = 71.5 and 85.3 ppm) differ significantly from those of **6** (δ = 79.7 ppm).

Table 3. Comparison between N···N and π···π distances [Å], as well as bond angles [°] at the nitrogen atom of **6**, [**6**·H]$^+$, [**6**·2H]$^{2+}$, **12**, [**12**·H]$^+$, [**6**·Ag]$^+$ and [**6**·Cu]$^+$.

	6	[**6**·H]$^+$	[**6**·2H]$^{2+}$	**12**	[**12**·H]$^+$	[**6**·Ag]$^+$	[**6**·Cu]$^+$
N···N	5.049(2)	4.247(1)	4.845(3)	6.14(4)	5.946(4)	4.622(2)	4.227(2)
π···π	3.760(2)	4.36(1)	3.94(1)	4.51(5)	4.557(4)	4.35(2)	4.34(2)
$\Sigma\omega_N$	344.7(2)	336.0(2)	336.3(2)	330.0(1)	333.0(2)	331.5(2)	326.4(8)

When an equimolar amount of TFAA was added to a solution of **12** in CH_2Cl_2, colorless crystals of [**12**·H]$^+$ were obtained within seconds. The signals of some of the aromatic protons of [**12**·H]$^+$ (δ = 6.80 ppm) are found at lower field than those of **12** (δ = 7.05 and 7.11 ppm). The shift difference in the ^{15}N NMR spectra of the protonated nitrogen atom of [**12**·H]$^+$ (δ = –306.1 ppm) and that of the nitrogen atoms of **12** (δ = –319.0 ppm) is smaller than that between [**6**·H]$^+$ and **6**. In the solid state [**12**·H]$^+$ adopts a helical shape with D_3 symmetry as well as a paddle-wheel shape with C_{3h} symmetry (Figure 3) in a disordered fashion, whereas in **12** only D_3 symmetry is encountered. It seems that the proton inside the cavity hinders the torsion of the benzene rings.

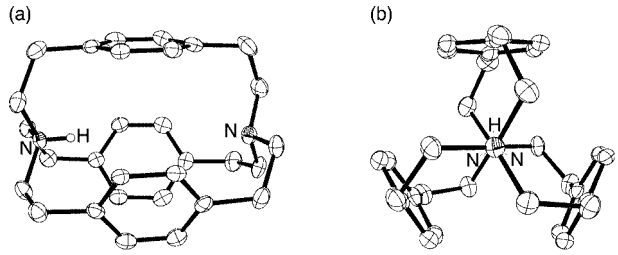

Figure 3. Molecular structure of [**12**·H]$^+$; a) side view; b) view along the N···N axis. Most hydrogen atoms and the anions are omitted for the sake of clarity.

Complexation with Silver(I) and Copper(I) Triflate

All seven π-prismands **6**–**12** were treated with silver(I) and copper(I) trifluoromethanesulfonate under argon in dry degassed dichloromethane at room temperature. After removal of the solvent, the complexes could be isolated as colorless stable materials. In all cases – except [**8**·Cu]$^+$ – we were able to grow single crystals which allowed us to carry out X-ray structural investigations. The Cu^I and Ag^I complexes of **6**[18] as well as the Ag^I complex of **12**[9] have been published in a preliminary account. In Table 4 selected distances and angles of **6**, **7**, and the metal complexes of **6**–**8** are listed. It is seen that incorporating a metal ion reduces the N···N distance. This is especially drastic in the series of **6**, [**6**·Ag]$^+$, [**6**·Cu]$^+$ and **7**, [**7**·Ag]$^+$, [**7**·Cu]$^+$, where the N···N distance is reduced by 0.8 Å and 0.6 Å, respectively. This shortening does not affect the individual bond lengths of adjacent atoms but the torsion of the bridges along the N···N axis and the distance between the π-units (see Table 3). This can be seen from Figure 4 where the protonated forms of **6** are compared with the corresponding silver and copper complexes.

The values found for the metal–nitrogen distances (2.23–2.39 Å for the Ag–N and 2.07–2.31 Å for the Cu–N distance) are close to those reported in the literature for (amine)silver(I)[20] and -copper(I)[20] complexes. In Table 4 are also listed the values found for the distances between the metal ion and the center of the triple bonds. For the silver complexes these values vary between 2.43 and 2.69 Å. These distances are close to those reported for various (alkyne)silver(I)[21] and -copper(I)[21b,22] complexes.

Table 4. Comparison of bond lengths and bond angles of **6**–**9** and their Ag^I and Cu^I complexes. The results of a DFT calculation on **8** are added in brackets.

	6[8]	[**6**·Ag]$^+$[9]	[**6**·Cu]$^+$[9]	**7**[8a]	[**7**·Ag]$^+$	[**7**·Cu]$^+$	**8**[e]	[**8**·Ag]$^+$	**9**	[**9**·Ag]$^+$	[**9**·Cu]$^+$
N···N [Å]	5.049(2)	4.622(5)	4.227(6)	4.662(2)	4.251(4)	4.020(7)	(4.541)[e]	4.435(2)	5.103(2)	4.737(3)	5.034(3)
N···M [Å][a]		2.311(3)	2.114(2)[d]		2.362(3)	2.089(6)		2.230(2)		2.389(2)	2.314(4)
					2.460(4)						2.722(4)
M···π [Å][b]		2.514(4)	2.461(4)					2.435(3)		2.479(2)	2.179(4)
			2.490(4)					2.505(3)		2.559(2)	
			2.576(4)							2.634(2)	
$\Sigma\omega_N$ [°][c]	344.7(2)	331.5(4)	326.4(3)[d]	341.1(3)	334.2(4)[d]	329.4(9)[d]	(336.9)[e]	332.1(3)	337.2(3)	328.2(3)	331.8(3)
d(C≡C) [Å]	1.118(2)	1.198(4)	1.191(6)	1.189(3)[d]	1.192(5)	1.19(1)	(1.207)[e]	1.198(4)	1.185(2)	1.196(3)	1.200(4)
							(1.208)[e]				

[a] Distances between nitrogen atoms and metal ion. [b] Distance between metal ion and center of π-system;. [c] Average bond angle at nitrogen atoms. [d] Average value. [e] Values derived from a DFT calculation on **8**.

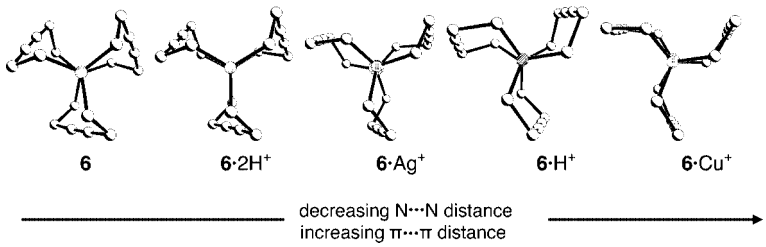

Figure 4. Conformations of prismand **6** depending on different complexations. The hydrogen atoms and the anions are omitted for the sake of clarity.

To address the question of an interaction between the triple bonds in **6**–**9** with the central metal ion we have first compared the ^{13}C NMR chemical shift of the sp-carbon signal of the complexed species with that of the parent cage compound (Table 5). The differences are small and no clear trend is obvious. More sensitivity was revealed by the stretching vibrations of the triple bonds recorded by means of Raman spectroscopy. They clearly show a strong shift towards smaller wavenumbers with complexation, indicating a weakening of the triple bonds. This can be rationalized by assuming a net transfer of electron density from the π-system to the metal ion of the triple bond. The net transfer is due to the fact that the electron donation of the triple bonds is stronger than the back donation of the metal ion. A stronger shift is found for the Ag^+ complexes than for the Cu^+ complexes. This stronger interaction of the Ag^+ ion with the triple bonds was ascribed to the larger radius of Ag^+ (1.26 Å) as compared to that of Cu^+ (0.96 Å).[23]

In Figure 5 the molecular structures of [**8**·Ag]$^+$ and [**9**·Ag]$^+$ are shown. In the first complex the N···N distance is by 0.30 Å shorter than in [**6**·Ag]$^+$, which indicates a higher flexibility in **8** due to the hexano bridge. The N–Ag distance in [**8**·Ag]$^+$ is 2.23 Å, a value close to that found for (amine)-silver complexes.[17,18] In [**9**·Ag]$^+$ a closer contact of the octyne bridge triple bond to the metal ion is found than of the two hexyne bridges (see also Table 4). This non-equal coordination between the triple bonds and Ag^+ results in a bending of the N–Ag–N axis to 165° (see Figure 5). In the X-ray structure of [**9**·Cu]$^+$ (see Table 4) the metal ion is disordered over two positions (84:16) which differ by 0.44 Å along the N···N axis. It seems that in **9** the N···N distance is too long for the small Cu^+ ion to coordinate both N atoms. The inclusion of Ag^+ into **10** reduces the N···N distance by 0.46 Å resulting in a bending of the benzene ring towards the outside (see Figure 6). The geometry of the complex [**10**·Ag]$^+$ is mainly determined by the interaction of the metal ion with the two nitrogen atoms and the triple bonds. The distances between the metal ion and the nitrogen centers and the triple bonds (see Table 6) are close to those reported for other (amine)Ag^+ complexes[19] and (alkyne)Ag^+ complexes.[21] The distance between the silver ion and the center of the benzene ring amounts to 2.68 Å (Table 6). This distance is shorter than those reported for an η^2-coordination of Ag^+ with benzene units (2.92 Å[24] and 3.01 Å[24]).

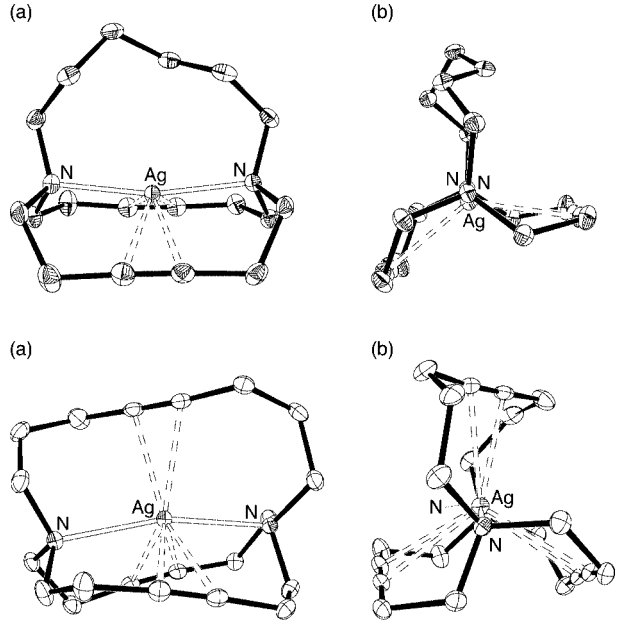

Figure 5. Molecular structures of [**8**·Ag]$^+$ (top) and [**9**·Ag]$^+$; a) side view; b) view along the N···N axis. The hydrogen atoms and the anions are omitted for the sake of clarity.

The interaction of the silver ion with the benzene ring causes a shift in the ^1H NMR spectra towards lower field by 0.39 ppm (see Table 7) with respect to the uncomplexed species. The strong complexation between the triple bonds and the silver ion shows up in a lowering of the stretching frequency by 36 cm^{-1} with respect to that of the ligand (Table 7).

Table 5. Comparison between the ^{13}C NMR spectroscopic data and the Raman data of **4**–**6** and their Ag^+ and Cu^+ complexes.

	6	[**6**·Ag]$^+$	[**6**·Cu]$^+$	**7**	[**7**·Ag]$^+$	[**7**·Cu]$^+$	**8**	[**8**·Ag]$^+$	[**8**·Cu]$^+$	**9**	[**9**·Ag]$^+$	[**9**·Cu]$^+$
^{13}C NMR [δ(sp-C)]	79.9	77.9	81.2	80.0	81.3	82.8	79.5	79.2	81.0	80.2	80.1 79.3	81.2 80.5
Raman [cm^{-1}]	2288 2227	2253 2187	2263 2201				2297 2231	2238 2176	2193	2297 2239	2263 2199	2230 2196

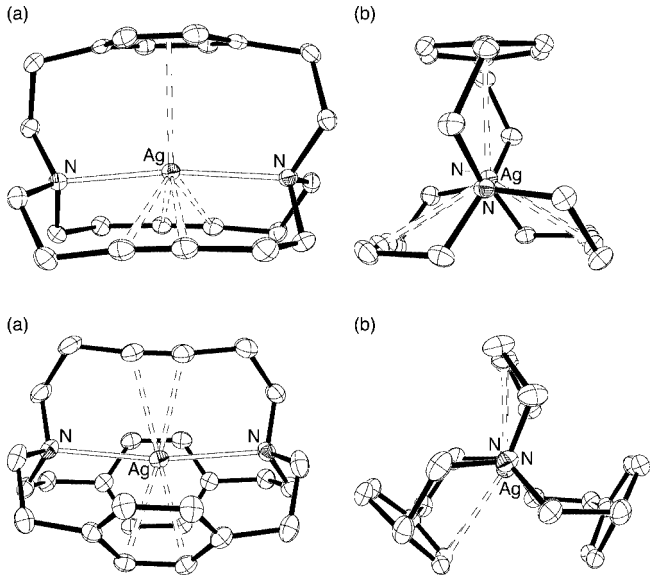

Figure 6. Molecular structures of [**10**·Ag]$^+$ (top) and [**11**·Ag]$^+$; a) side view; b) view along the N···N axis. The hydrogen atoms and the anions are omitted for the sake of clarity.

Table 6. Selected geometrical parameters of the silver complexes [**10**·Ag]$^+$ to [**12**·Ag]$^+$.

	[**10**·Ag]$^+$	[**11**·Ag]$^+$	[**12**·Ag]$^+$
N···N [Å]	4.837(3)	5.203(3)	5.979(4)
N···Ag [Å]	2.418(2)	2.581(2)	2.462(3)
	2.431(2)	2.639(2)	3.516(3)
π···Ag [Å][a]	2.522(2)	2.530(3)	
	2.556(2)		
π(Ar)···Ag [Å][b]	2.679(2)	2.710(3), 2.739(3)	2.700(3)
C_{Ar}···Ag [Å][c]	2.983(2)	2.730(3)	2.536(2)
N···Ag···N [°]	172.0(1)	170.8(1)	180.0

[a] Distance between the center of the triple bond and the metal ion. [b] Distance between the center of the benzene rings and the metal ion. [c] Shortest distance between a carbon atom of the benzene ring and the metal ion.

Table 7. Comparison of spectroscopic data of **10**–**12** and their silver complexes.

	10	[**10**·Ag]$^+$	**11**	[**11**·Ag]$^+$	**12**[9]	[**12**·Ag]$^+$[9]
^{1}H NMR [δ(H_{Ar})]	7.06	7.45	6.85, 7.02	7.19, 7.45	6.57	6.89
^{13}C NMR [δ(sp-C)]	78.1	78.0	77.0	78.0		
Raman [cm^{-1}]	2231	2195	2222	2184		

In the silver complex of **11** the N···N distance is reduced by 0.43 Å with respect to the N···N distance calculated for the free ligand, but it is larger than that found for [**10**·Ag]$^+$ due to the presence of two rigid benzene rings; this leads to a longer N–Ag distance. As seen from the molecular structure of [**11**·Ag]$^+$ in Figure 6, the butyne unit is bent (12.2°) towards the metal ion. One of the benzene rings is η^2-coordinated, all the other sp^2-carbon atoms are away from the metal ion by about or more than 3 Å. In solution two signals are found in the ^{1}H NMR spectrum for the aromatic protons. Both are shifted towards lower field by 0.34 and 0.43 ppm as compared to those of the free ligand (see Table 7). The shift of the stretching frequency of the triple bonds amounts to 38 cm^{-1}, indicating the anticipated strong interaction between Ag$^+$ and the alkyne unit.

The silver complex of **12** has been published in a preliminary account.[9] In the meantime we have obtained better data which are listed in Table 6. The silver ion is disordered along the N···N axis; due to the relative long N···N distance in **12** (6.14 Å) a symmetrical position is less favored than an unsymmetrical one. The shorter N–Ag distance amounts to 2.46 Å, it is still longer than that found in [**6**·Ag]$^+$ (2.31 Å). This difference can be ascribed to a rather strong interaction between the silver ion and the π-system in [**12**·Ag]$^+$. Indeed, all three benzene rings are tilted in a conrotatory fashion towards the silver ion. As a result, the distance between the metal ion and one sp^2-carbon atom of each ring amounts to 2.54 Å. When the fact is considered that two neighboring sp^2-centers at each ring also come close to the silver ion (2.77 Å and 2.82 Å, respectively) an η^3-coordination between the metal ion and the three benzene rings results. The strong arene–metal interaction compensates the weak interaction between the second nitrogen center and the metal ion (3.52 Å).

There are two ways of interpreting the distribution of the metal ion in **12** on two equivalent positions on the N···N axis: Either a fluctuation between both takes place or there is a spatial disorder in the crystal lattice. We favour a spatial disorder because we assume an interaction between the silver cation and the orientation of the triflate anion which are fixed in the solid state. The NMR spectra of [**12**·Ag]$^+$ (Figure 7) in CD_2Cl_2 might be compatible with D_3 symmetry at room temperature. Below the coalescence temperature at 0 °C we find a splitting of the signals of the aromatic protons and those CH_2 groups adjacent to the nitrogen atoms. In the ^{13}C NMR spectrum at –50 °C a doubling of the signals of the methylene groups is observed (see Figure 8). This result might be rationalized by a preferred coordination of the metal ion to one of the nitrogen centers. However, the difference in the intensity of the ^{1}H and ^{13}C signals in the aromatic region (see Figure 8) is not in line with this interpretation. The pattern found resembles that found for the uncomplexed π-prismands. It can also be rationalized by a freezing of the isomerization of one helical conformation (D_3) to the other by a paddle-wheel conformation (C_{3h}) as shown in Figure 1. The inclusion of the metal ion increases the activation energy of this process. Below the coalescence temperature (0 °C) we were able to detect two different conformations of a lower symmetry than (D_3) of which one (signals 1–4) is more favored than the other (signals 1′–4′) as shown in Figure 8. This result can be rationalized by a simultaneous slowing down of the torsional movement of the bridges and a retardation of the torsional movement of the benzene rings which leads to the doubling of the signals. Below 0 °C the aromatic rings are fixed in a lateral position which is favored by a threefold η^3-coordination with the silver ion. Depending on which signal splitting we based our calculations on (38–312 Hz), we estimated the activation enthalpy for the movement of

the bridges to 12.4–13.5 kcal/mol. The simultaneous fluctuation of the metal ion could not be frozen out down to –100 °C.

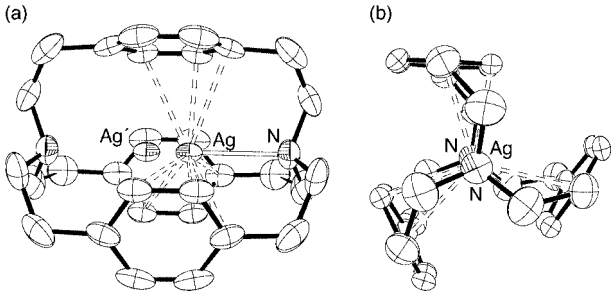

Figure 7. Molecular structures of [**12**·Ag]$^+$; a) side view; b) view along the N···N axis. The hydrogen atoms and the anion is omitted for the sake of clarity.

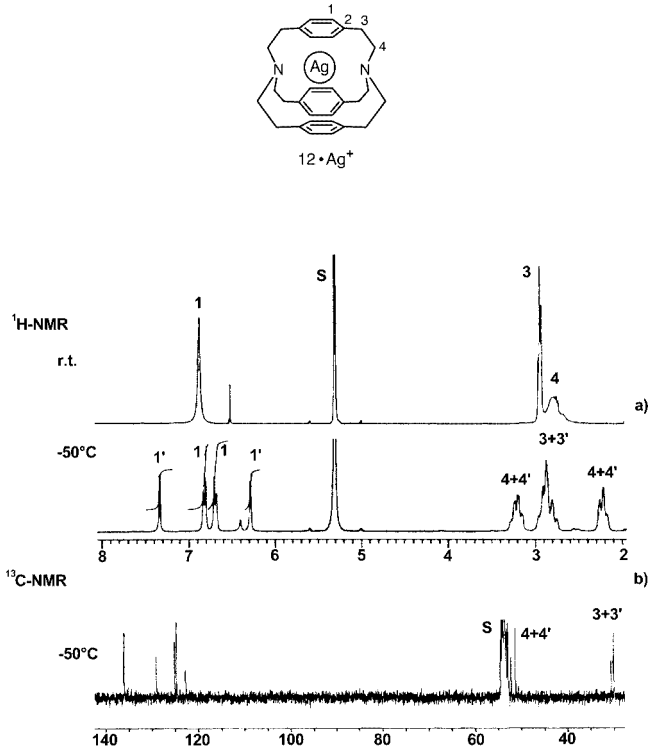

Figure 8. a) ^{1}H NMR spectra of [**12**·Ag]$^+$ at room temperature and at –50 °C; b) ^{13}C NMR spectrum of [**12**·Ag]$^+$ at –50 °C.

The arrangement of the benzene rings in [**12**·Ag]$^+$ is reminiscent of the topology of the silver complexes with [2$_3$](1,4)cyclophane **15**[7] and [2$_6$](1,2,4,5)cyclophane **16**[24] in so far as both cyclophanes form complexes with Ag$^+$ in which the metal ion is not situated in the center of the cavity but somewhat shifted to the periphery. In [**15**·Ag]$^+$ a threefold η^2-coordination results with a shortest C(sp^2)–Ag distance of 2.59 Å. In the case of [**16**·Ag]$^+$ the silver ion is threefold η^2-coordinated [C(sp^2)–Ag = 2.43 Å]. In both cases the anions are associated with the cation. Here, we also mention concave macrocycles[25,26] in which four to seven benzene rings form a cavity. For these species a selective complexation of silver ions was shown.[25,26] In [**12**·Ag]$^+$ one nitrogen atom takes the function of the anions in [**15**·Ag·CF_3SO_3][7] and [**16**·Ag·CF_3SO_3].[24]

The signals of the aromatic protons in the complex [**12**·Ag]$^+$ are shifted towards lower field (Table 7) as already encountered in the cases of [**11**·Ag]$^+$ and [**10**·Ag]$^+$. This might be ascribed to a transfer of electron density from the π-system to the metal ion.[25] On the other hand this shift might also be caused by a mutual shielding of the aromatic protons due to the restricted torsional rotation of the benzene moieties. However, the shift of the aromatic hydrogen atoms in [**10**·Ag]$^+$ as compared to **10** (Table 7) favours a strong metal effect.

The copper(I) salts of **10**–**12** could be prepared. In the case of [**10**·Cu]$^+$ we were able to grow single crystals but its structural elucidation caused problems. Similarly to [**12**·Ag]$^+$, crystals suffered from a phase transition on cooling, so that the structure could only be determined at room temperature. At this temperature a disorder was found which allowed no detailed investigation. However, it can be deduced that the metal ion is encapsulated in the ligand cavity, and its position is unsymmetrical with respect to the nitrogen atoms. Further evidence on the bonding relations in [**10**·Cu]$^+$ was obtained from spectroscopic data. The signal of the aromatic protons (δ = 7.26 ppm) is less shifted towards lower field than that of [**10**·Ag]$^+$ (δ = 7.45 ppm). A strong shift towards lower field can be observed for the sp-C signal (δ = 82.8 ppm) as compared to that of **10** (δ = 78.1 ppm). This shows a strong interaction between Cu$^+$ and the alkyne units. In line with this interpretation is a strong reduction of the stretching vibration as found in the Raman spectrum of [**10**·Cu]$^+$ (δ = –81 cm^{-1}). The spectroscopic data of [**11**·Cu]$^+$ suggest similar interactions between

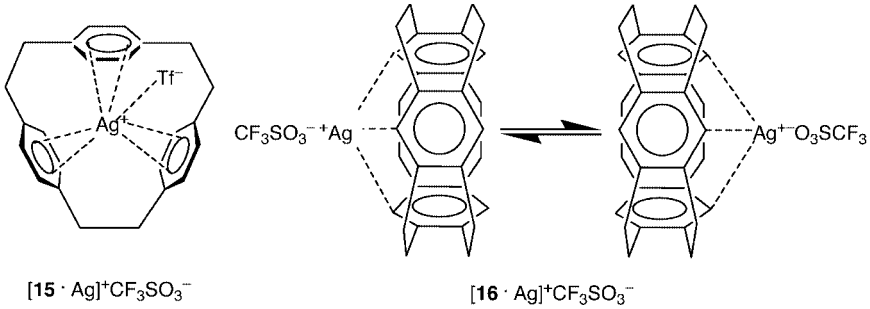

the metal ion and the ligand (Table 8). In the case of [**12**·Cu]$^+$, we were able to carry out an X-ray study on a single crystal, again only at room temperature due to a phase transition on cooling. The metal ion is clearly fixed on one side of the cavity (see Figure 9). The smaller N–Cu distance amounts to 2.10 Å and is close to those values found in (amine)Cu$^+$ complexes (2.01–2.34 Å),[20] the longer Cu···N distance was found to be 4.06 Å. The close coordination of the metal ion with one nitrogen atom leads to a threefold η^2-coordination with the benzene rings in [**12**·Cu]$^+$. An η^2-coordination between benzene and Cu$^+$ has also been encountered in C_6H_6·$CuAlCl_4$.[27]

Table 8. Comparison of spectroscopic data of the copper(I) complexes of **10**–**12**.

	[**10**·Cu]$^+$	[**11**·Cu]$^+$	[**12**·Cu]$^+$
^{1}H NMR [δ(H_{Ar})]	7.26	7.16, 7.19	6.68
^{13}C NMR [δ(sp-C)]	82.8	82.4	
Raman [cm^{-1}]	2150	2124	

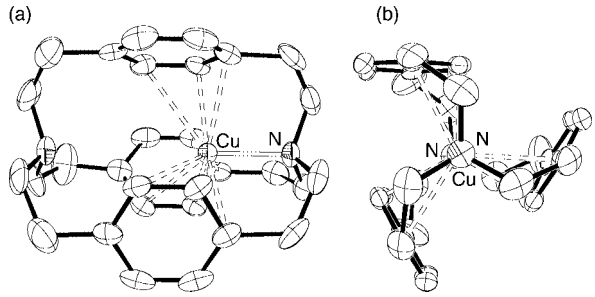

Figure 9. Molecular structure of [**12**·Cu]$^+$; a) side view; b) view along the N···N axis. The hydrogen atoms and the anion (triflate) are omitted for the sake of clarity.

In the ^{1}H NMR spectrum of [**12**·Cu]$^+$ we find two coalescence temperatures. Below 10 °C the broad singlet at δ = 7.26 ppm splits into two signals, which again split at –30 °C into four broad signals (Figure 10) that finally sharpen at –70 °C. In the ^{13}C NMR spectrum, we find a doubling of the signals of the CH_2 groups and the signal of

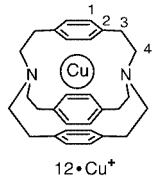

12•Cu$^+$

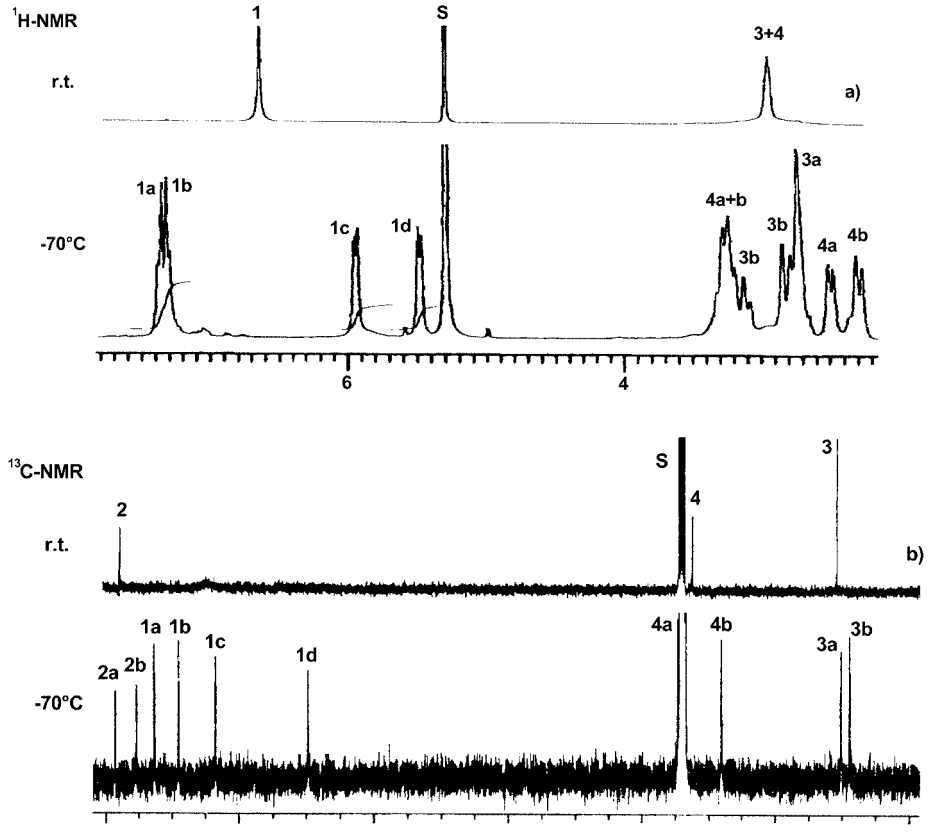

Figure 10. a) ^{1}H NMR spectra of [**12**·Cu]$^+$ at room temperature and at –70 °C; b) ^{13}C NMR spectra of [**12**·Cu]$^+$ at room temperature and at –70 °C.

the quaternary aromatic C atom (2a, 2b in Figure 10b). Below –40 °C the broad signal of the tertiary aromatic carbon atoms splits up into four peaks (1a–1d in Figure 10). These results suggest that the first point of coalescence is due to a slowing down of the torsional motion of the benzene rings. Below –30 °C a freezing of the metal ion fluctuation starts leading to C_3 symmetry. The threefold η^1-coordination of the Cu^+ ion leads to a further splitting of the ^1H and ^{13}C resonances in the aromatic regions. Based on the splitting of the ^1H signals in the aromatic region we can estimate for the rotation of the benzene rings (T_c = 10 °C, $\Delta\nu$ = 49 Hz) $\Delta G_c^{\#}$ = 14 kcal/mol. For the fluctuation of the metal ion (T_c = –30 °C, $\Delta\nu$ = 590 Hz) we obtain $\Delta G_c^{\#}$ = 11 kcal/mol.

Conclusions

The molecules **6**–**12** provide an interesting series of simple π-prismands with bridgehead nitrogen atoms and alkyne or benzene units in the bridges. All structurally characterized prismands adopt an *in*/*in* conformation. The different lengths of the bridges imply that the distances between the bridgehead atoms vary between 5.05 Å (**6**) and 6.15 Å (**12**). The cavity itself proved to be flexible and can adopt a helical (D_3) and a paddle-wheel (C_{3h}) conformation. This cavity allows the inclusion of protons and metal ions. For **6** a twofold protonation was found. For all seven π-prismands we observed the inclusion of copper(I) and silver(I) ions. A detailed investigation of the metal complexes did not only reveal the anticipated interaction between the metal ions and the bridgehead nitrogen atoms, but also an interaction with the triple bonds and the benzene rings. In the case of larger N···N distances (> 5.2 Å) the captured ion adopts an unsymmetrical position, i.e. it is closer to one nitrogen atom than to the other. This trend is reinforced when the larger silver ion is replaced by the smaller copper ion.

Experimental Section

General Remarks: All reactions were carried out under argon with magnetic stirring in dry degassed solvents. The ^1H and ^{13}C NMR spectra were recorded with Bruker AS 200 and WH 300 spectrometers. High-resolution mass spectra (HRMS) were obtained with a ZAB high-resolution mass spectrometer (Vacuum Generators). Micro analyses were performed at the Analytical Laboratory of the Chemische Institute der Universität Heidelberg. The preparation of **6**–**8** has been described earlier.[8]

General Procedure for the Three-Component Reaction: Three equiv. of α,ω-dibromoalkyne and one equiv. of α,ω-diaminoalkyne were refluxed in dry acetonitrile in the presence of 5–6 equiv. of powdered, dry potassium carbonate for 4–5 d. After cooling, the potassium carbonate was filtered off and the solvent was removed in vacuo. The residue was dissolved and purified by column chromatography.

Preparation of 1,10-Diazabicyclo[8.6.6]docosa-5,13,19-triyne (9): Starting materials: 1,6-dibromohex-3-yne (1.52 g, 6.3 mmol),[10] 1,8-diaminooct-4-yne,[11] (0.36 g, 2.5 mmol), powdered K_2CO_3 (15 g, 108 mmol) and 500 mL of acetonitrile. The residue was absorbed and chromatographed on ALOX III using petroleum ether/diethyl ether as solvent in the ratio of 5:1. After removal of the solvent, 0.22 g (29%) of **9** was obtained as a colorless solid; m.p. 156 °C. ^1H NMR (300 MHz, $CDCl_3$): δ = 1.67 (pseudo-quint, 4 H, CH_2), 2.26 (t, 8 H, CH_2–C≡), 2.32–2.49 (m, 4 H, CH_2–C≡, 8 H, CH_2–N), 2.55 (t, 4 H, CH_2–N) ppm. ^{13}C NMR (75 MHz, $CDCl_3$): δ = 15.7 (2 C, *C*H_2–C≡), 18.3 (4 C, *C*H_2–C≡), 25.5 (CH_2), 50.6 (2 C, CH_2–N), 52.0 (4 C, CH_2–N), 80.2 (6 C, C≡C) ppm. HRMS (EI+): $^{12}C_{20}{}^1H_{28}{}^{14}N_2$: calcd. 296.2253; found 296.2216; $^{12}C_{20}{}^1H_{27}{}^{14}N_2$: calcd. 295.2174; found 295.2177. IR (KBr): $\tilde{\nu}$ = 2963 (m), 2936 (m), 2899 (s), 2871 (m), 2794 (vs), 2750 (w), 1455 (m), 1420 (m), 1374 (m), 1336 (m), 1283 (m), 1133 (m), 1049 (m), 993 (m), 723 (w), 549 (w) cm^{-1}. $C_{20}H_{28}N_2$ (296.46): calcd. C 81.03, H 9.52, N 9.45; found C 81.00, H 9.72, N 9.35.

17-(1,4)Benzena-1,8-diazabicyclo[6.6.5]nonadecaphane-4,11-diyne (10): Starting materials: 1,6-dibromohex-3-yne[10] (540 mg, 2.3 mmol), 1,4-bis(2-aminoethyl)benzene[27] (181 mg, 1.1 mmol), powdered potassium carbonate (10 g, 73 mmol) and 350 mL of dry acetonitrile. The excess of potassium carbonate was filtered off. After removal of the solvent and chromatography on ALOX III with petroleum ether 30/40 and finally with cyclohexane/ethyl acetate (10:1), we obtained a colorless solid which was further purified by kugelrohr distillation. These procedures yielded 64 mg (18%) of **10** as colorless powder, m.p. 114 °C. ^1H NMR (300 MHz, $CDCl_3$): δ = 2.15–2.32 (m, 16 H, CH_2–C≡, CH_2–N), 2.61 (t, ^3J = 6.3 Hz, 4 H, CH_2–Ar), 2.76 (t, ^3J = 6.3 Hz, 4 H, CH_2–N), 7.06 (s, 4 H, H_{ar}) ppm. ^{13}C NMR (75 MHz, $CDCl_3$): δ = 17.7 (*C*H_2–C≡), 32.3 (CH_2–Ar), 50.9 (CH_2–N), 54.1 (CH_2–N), 78.1 (C≡C), 127.8 (t-C_{ar}), 136.4 (q-C_{ar}) ppm. HRMS (FAB+): $^{12}C_{22}{}^1H_{28}{}^{14}N_2{}^{23}Na$: calcd. 343.2151; found 343.2165; $^{12}C_{22}{}^1H_{29}{}^{14}N_2$: calcd. 321.2330; found 321.2348; $^{12}C_{22}{}^1H_{27}{}^{14}N_2$: calcd. 319.2174; found 319.2201. IR (KBr): $\tilde{\nu}$ = 3009 (w), 2981 (m), 2950 (s), 2895 (s), 2784 (vs), 2731 (s), 2644 (m), 2097 (br., w), 1452 (s), 1377 (s), 1267 (s), 1231 (s), 1131 (s), 1032 (s), 802 (s), 599 (m) cm^{-1}. $C_{22}H_{28}N_2$ (320.48): calcd. C 82.45, H 8.81, N 8.74; found C 82.41, H 8.84, N 8.73.

11,16-(1,4)Dibenzena-1,8-diazabicyclo[6.5.5]octadecaphan-4-yne (11): Starting materials: 1,4-bis(2-bromoethyl)benzene[28] (380 mg, 1.3 mmol), 1,6-diaminohex-3-yne[9] (61 mg, 0.5 mmol), powdered potassium carbonate (4 g, 29 mmol), 100 mL of dry acetonitrile. After removal of the solvent and chromatography on ALOX III with cyclohexane/ethyl acetate (5:1), we obtained 180 mg (89%) of **11** as colorless oil, which crystallized after a few hours, m.p. 107 °C. ^1H NMR (300 MHz, $CDCl_3$): δ = 2.03–2.10 (m, 8 H, CH_2–C≡, CH_2–N), 2.43–2.83 (m, 16 H, CH_2–N, CH_2–Ar), 6.85 (s, 4 H, H_{ar}), 7.02 (s, 4 H, H_{ar}) ppm. ^{13}C NMR (75 MHz, $CDCl_3$): δ = 17.1 (*C*H_2–C≡), 32.2 (CH_2–Ar), 49.0 (CH_2–N), 53.0 (CH_2–N), 77.0 (C≡C), 127.2 (t-C_{ar}), 128.8 (t-C_{ar}), 136.2 (q-C_{ar}) ppm. HRMS (FAB+): $^{12}C_{26}{}^1H_{32}{}^{14}N_2{}^{23}Na$: calcd. 395.2463; found 395.2489; $^{12}C_{26}{}^1H_{33}{}^{14}N_2$: calcd. 373.2644; found 373.2650; $^{12}C_{26}{}^1H_{31}{}^{14}N_2$: calcd. 371.2488; found371.2509. IR (film): $\tilde{\nu}$ = 3011 (m), 2901 (s), 2852 (s), 2786 (vs), 2734 (s), 1515 (m), 1452 (s), 1379 (s), 1224 (s), 1129 (s), 1029 (m), 794 (s), 734 (m), 600 (m) cm^{-1}. $C_{26}H_{32}N_2$ (372.55): calcd. C 83.83, H 8.66, N 7.52; found C 83.50, H 8.35, N 7.49.

4,10,15-(1,4)Tribenzena-1,7-diazabicyclo[5.5.5]heptadecaphane (12): Starting materials: 1,4-bis(2-bromoethyl)benzene[28] (657 mg, 2.3 mmol), 1,4-bis(2-aminoethyl)benzene[29] (181 mg, 1.1 mmol), powdered potassium carbonate (10 g, 73 mmol) and 400 mL of dry acetonitrile. After 5 d of refluxing, the excess of potassium carbonate was separated by filtration. After removal of the solvent, the residue was chromatographed on ALOX III with petroleum ether 30/40 yielding 62 mg (13%) of colorless crystals; m.p. 162 °C. ^1H

NMR (500 MHz, $CDCl_3$): δ = 2.69 (br. s, 12 H, CH_2–N), 2.78 (t, ^3J = 5.8 Hz, 12 H, CH_2–Ar), 6.57 (s, 12 H, H_{ar}) ppm. ^{13}C NMR (125 MHz, $CDCl_3$): δ = 32.2 (CH_2–Ar), 52.7 (CH_2–N), 128.8 (t-C_{ar}), 136.6 (q-C_{ar}) ppm. HRMS(FAB+): $^{12}C_{30}{}^{1}H_{37}{}^{14}N_2$: calcd. 425.2957; found 425.2966; $^{12}C_{30}{}^{1}H_{36}{}^{14}N_2$: calcd. 424.2879; found 424.2908. IR (KBr): $\tilde{\nu}$ = 3049 (w), 3006 (w), 2960 (vs), 2920 (s), 2858 (s), 2779 (vs), 2730 (s), 1514 (m), 1451 (s), 1379 (m), 1264 (m), 1218 (m), 1125 (s), 1097 (s), 1024 (s), 797 (vs), 741 (m), 601 (m) cm^{-1}. $C_{30}H_{36}N_2$ (424.63): calcd. C 84.86, H 8.55, N 6.60; found C 84.23, H 8.41, N 6.61.

General Procedure for the Preparation of $[6\cdot H]^+$ and $[12\cdot H]^+$: We investigated the protonation of **6** in $CDCl_3$ and CD_3OD by means of NMR spectroscopy. To generate the monoprotonated $[6\cdot H]^+$ in $CDCl_3$, 3 equiv. of trifluoroacetic acid (TFAA) were required. In CD_3OD only 1 equiv. of TFAA was necessary. The diprotonation of **6** has already been reported in the literature.[18] The protonation of **12** was achieved in CD_2Cl_2 and CD_3OD at room temperature with 1 equiv. of TFAA.

$[6\cdot H]^+$: ^1H NMR (300 MHz, $CDCl_3$): δ = 2.41 (m, 12 H), 2.80 (m, 6 H, CH_2), 3.42 ppm (m, 6 H, CH_2–NH) ppm. ^{13}C NMR (75 MHz, $CDCl_3$): δ = 15.0 (*C*H_2–C≡), 17.0 (*C*H_2–C≡), 50.1 (*C*H_2–N), 50.2 (*C*H_2–NH^+), 70.1 (sp-C), 86.1 (sp-C) ppm.

$[12\cdot H]^+$: ^1H NMR (500 MHz, CD_3OD): δ = 2.72 (m, 6 H), 3.00 (m, 6 H), 3.21 (m, 6 H), 3.46 (m,6 H), 6.80 (m, 6 H), 7.25 ppm (m, 6 H) ppm. ^{13}C NMR (125.8 MHz, CD_3OD): δ = 29.8, 32.6, 53.2, 55.4, 129.5, 130.7, 132.3, 140.7 ppm.

General Procedure for the Preparation of the Silver(I) and Copper(I) Triflates of 6–12: The operations were carried out in a glove box under argon. The reactions were carried out in a Schlenk apparatus. To the silver triflate was added the ligand and dry degassed dichloromethane. For the preparation of the Cu^I complexes we used the benzene complex of copper(I) triflate. As reaction medium we used dichloromethane in both cases. The mixture was stirred at room temperature for about 3 h. The reaction flask was protected with aluminum foil to exclude light. After removal of the solvent in vacuo, the complexes were obtained in quantitative yield.

(1,8-Diazabicyclo[6.6.6]eicosa-4,11,17-triyne)silver(I) Trifluoromethanesulfonate ($[6\cdot Ag^+][CF_3SO_3]^-$): Starting materials: **6** (50 mg, 1.9 mmol), silver(I) triflate (50 mg, 0.2 mmol), and 10 mL of dry, degassed dichloromethane. After removal of the solvent, we obtained 99 mg (100%) of $[6\cdot Ag^+][CF_3SO_3]^-$ as colorless powder, m.p. 235 °C (dec.). ^1H NMR (500 MHz, $CDCl_3$): δ = 2.58 (t, ^3J = 5.3 Hz, 12 H, CH_2–C≡), 2.68 (pseudo-quint, 12 H, CH_2–N) ppm. ^{13}C NMR (125 MHz, $CDCl_3$): δ = 18.2 (*C*H_2–C≡), 52.8 (CH_2–N), 77.9 (C≡C) ppm. HRMS (FAB+): $^{12}C_{18}{}^{1}H_{24}{}^{109}Ag^{14}N_2$: calcd. 377.0987; found 377.0977; $^{12}C_{18}{}^{1}H_{24}{}^{107}Ag^{14}N_2$: calcd. 375.0990; found 375.0986. IR (KBr): $\tilde{\nu}$ = 2936 (w), 2892 (w), 2865 (w), 2808 (m), 1651 (w), 1457 (m), 1431 (w), 1378 (w), 1333 (w), 1264 (vs), 1228 (s), 1154 (s), 1031 (vs), 966 (w), 803 (m), 638 (s) cm^{-1}. $C_{19}H_{24}AgF_3N_2O_3S$ (525.34): calcd. C 43.44, H 4.60, N 5.33; found C 43.06, H 4.67, N 5.24.

(1,8-Diazabicyclo[6.6.5]nonadeca-4,11-diyne)silver(I) Trifluoromethanesulfonate ($[7\cdot Ag]^+[CF_3SO_3]^-$): Starting materials: **7** (29 mg, 0.1 mmol), silver(I) triflate (27 mg, 0.1 mmol) and 15 mL of dry, degassed dichloromethane. After removal of the solvent, the residue was recrystallized from chloroform to yield 46.5 mg (83%) of $[7\cdot Ag]^+[CF_3SO_3]^-$ as colorless powder; m.p. 220 °C (dec.). ^1H NMR (500 MHz, CD_3OD): δ = 1.65–1.71 (m, 4 H, $2CH_2$), 1.98 (quint, ^3J = 7.1 Hz, 2 H, CH_2), 2.57–2.67 (m, 8 H, CH–C≡), 2.72–2.82 (m, 12 H, CH_2–N) ppm. ^{13}C NMR (125 MHz, CD_3OD): δ = 20.7, 23.1, 27.7, 52.8, 57.4, 81.3 ppm. IR (KBr): $\tilde{\nu}$ = 2904, 2791, 1458, 1259, 1169, 1040 cm^{-1}. HRMS (positive FAB): $C_{17}H_{26}{}^{107}AgN_2$: calcd. 365.1132, found 365.1125; $C_{17}H_{26}{}^{109}AgN_2$: calcd. 367.1158, found 367.1136.

(1,8-Diazabicyclo[6.6.6]eicosa-4,11-diyne)silver(I) Trifluoromethanesulfonate ($[8\cdot Ag]^+[CF_3SO_3]^-$): Starting materials: **8** (29 mg, 0.1 mmol), silver(I) triflate (27 mg, 0.1 mmol) and 15 mL of dry, degassed dichloromethane. After removal of the solvent, we obtained 56 mg (100%) of $[8\cdot Ag]^+[CF_3SO_3]^-$ as colorless powder, m.p. 164 °C (dec.). ^1H NMR (500 MHz, CD_2Cl_2): δ = 1.75 (s, 4 H, N–CH_2–C*H*$_2$–CH_2), 1.83 (s, 4 H, N–CH_2–CH_2–C*H*$_2$), 2.67 (s, 8 H, CH_2–C≡, 4 H, N–C*H*$_2$–CH_2–CH_2), 2.75 (s, 8 H, CH_2–N) ppm. ^{13}C NMR (125 MHz, CD_2Cl_2): δ = 19.0 (CH_2–C≡), 26.0 (N–CH_2–*C*H_2–CH_2), 26.8 (N–CH_2–CH_2–*C*H_2), 53.9 (N–*C*H_2–CH_2–CH_2), 55.2 (N–*C*H_2–CH_2–C≡), 79.2 (C≡C) ppm. HRMS (FAB+): $^{12}C_{18}{}^{1}H_{28}{}^{109}Ag^{14}N_2$: calcd. 381.1300; found 381.1276; $^{12}C_{18}{}^{1}H_{28}{}^{107}Ag^{14}N_2$: calcd. 379.1304, found 379.1297. IR (KBr): $\tilde{\nu}$ = 2962 (m), 2906 (m), 2787 (m), 1457 (w), 1262 (vs), 1099 (s), 1034 (s), 803 (s), 652 (m) cm^{-1}.

(1,10-Diazabicyclo[8.6.6]docosa-5,13,19-triyne)silver(I) Trifluoromethanesulfonate ($[9\cdot Ag]^+[CF_3SO_3]^-$): Starting materials: **9** (20 mg, 0.07 mmol), silver(I) triflate (18 mg, 0.07 mmol) and 5 mL of dry, degassed dichloromethane. After removal of the solvent, we obtained 38 mg (100%) of $[9\cdot Ag]^+[CF_3SO_3]^-$ as colorless powder, m.p. 185 °C (dec.). ^1H NMR (500 MHz, CD_3OD): δ = 1.80 (pseudo-quint, 4 H, CH_2–C*H*$_2$–CH_2), 2.48–2.61 (m, 20 H, CH_2–N, CH_2–C≡), 2.72 (m, 4 H, CH_2–N). ^{13}C NMR (125 MHz, CD_3OD): δ = 18.3 (*C*H_2–C≡), 18.6 (*C*H_2–C≡), 25.2 (CH_2–*C*H_2–CH_2), 54.7 (CH_2–N), 56.3 (CH_2–N), 79.3 (4 C, C≡C), 80.1 (2 C, C≡C) ppm. HRMS (FAB+): $^{12}C_{20}{}^{1}H_{28}{}^{109}Ag^{14}N_2$: calcd. 405.1300; found 405.1317; $^{12}C_{20}{}^{1}H_{28}{}^{107}Ag^{14}N_2$: calcd. 403.1304; found 403.1305. IR (KBr): $\tilde{\nu}$ = 2962 (w), 2934 (m), 2900 (m), 2794 (m), 1458 (m), 1272 (vs), 1146 (s), 1033 (s), 639 (s), 519 (w) cm^{-1}.

{17-(1,4)Benzena-1,8-diazabicyclo[6.6.5]nonadecaphane-4,11-diyne}silver(I) Trifluoromethanesulfonate ($[10\cdot Ag]^+[CF_3SO_3]^-$): Starting materials: **10** (25 mg, 0.08 mmol), silver(I) triflate (20 mg, 0.08 mmol) and 5 mL of dry, degassed dichloromethane. After removal of the solvent, we obtained 45 mg (100%) of $[10\cdot Ag]^+[CF_3SO_3]^-$ as a colorless powder, m.p. 290 °C (dec.). ^1H NMR (300 MHz, CD_2Cl_2): δ = 2.33–2.56 (m, 12 H, N–C*H*$_2$–C*H*$_2$–C≡), 2.77 (m, 4 H, CH_2–N), 3.05 (t, ^3J = 6.4 Hz, 4 H, CH_2–Ar), 7.45 (s, 4 H, H_{ar}) ppm. ^{13}C NMR (75 MHz, CD_2Cl_2): δ = 17.3 (*C*H_2–C≡), 31.5 (CH_2–Ar), 51.9 (N–*C*H_2–CH_2–C≡), 55.1 (CH_2–N), 78.0 (C≡C), 129.1 (t-C_{ar}), 135.6 (q-C_{ar}) ppm. HRMS (FAB+): $^{12}C_{22}{}^{1}H_{28}{}^{109}Ag^{14}N_2$: calcd. 429.1300; found 429.1313; $^{12}C_{22}{}^{1}H_{28}{}^{107}Ag^{14}N_2$: calcd. 427.1303; found 427.1288.

{11,16-(1,4)Dibenzena-1,8-diazabicyclo[6.5.5]octadecaphane-4-yne}silver(I) Trifluoromethanesulfonate ($[11\cdot Ag]^+[CF_3SO_3]^-$): Starting materials: **11** (25 mg, 0.07 mmol), silver(I) triflate (17 mg, 0.07 mmol) and 5 mL of dry, degassed dichloromethane. After removal of the solvent, we obtained 42 mg (100%) of $[11\cdot Ag]^+[CF_3SO_3]^-$ as a colorless powder, m.p. 250 °C (dec.). ^1H NMR (500 MHz, CD_2Cl_2): δ = 2.23 (s, 4 H, N–C*H*$_2$–CH_2–C≡), 2.37 (t, ^3J = 5.6 Hz, 4 H, CH_2–C≡), 2.48–2.53 (m, 4 H, CH_2–Ar), 2.83–2.89 (m, 8 H, N–C*H*$_2$–C*H*$_2$–Ar), 3.01–3.06 (m, 4 H, CH_2–N), 7.19 (s, 4, H_{ar}), 7.45 (s, 4, H_{ar}) ppm. ^{13}C NMR (125 MHz, CD_2Cl_2): δ = 17.0 (d, $^2J_{C,Ag}$ = 1.9 Hz, *C*H_2–C≡), 31.5 (CH_2–Ar), 49.5 (N–*C*H_2–CH_2–C≡), 54.9 (N–*C*H_2–CH_2–Ar), 78.0 (d, $^1J_{C,Ag}$ = 4.7 Hz, C≡C), 127.9 (t-C_{ar}), 130.0 (t-C_{ar}), 136.4 (q-C_{ar}) ppm. HRMS (FAB+): $^{12}C_{26}{}^{1}H_{32}{}^{109}Ag^{14}N_2$: calcd. 481.1613; found 481.1607; $^{12}C_{26}{}^{1}H_{32}{}^{107}Ag^{14}N_2$: calcd. 479.1616; found 479.1604. IR (KBr): $\tilde{\nu}$ = 2826 (m), 1513 (w), 1452 (m), 1270 (vs), 1226 (s), 1155 (s), 1033 (s), 815 (m), 740 (w), 639 (s) cm^{-1}.

{4,10,15-(1,4)Tribenzena-1,7-diazabicyclo[5.5.5]heptadecaphane}-silver(I) Trifluoromethanesulfonate ([12·Ag]$^+$[CF_3SO_3]$^-$): Starting materials: **12** (25 mg, 0.06 mmol), silver(I) triflate (17 mg, 0.07 mmol) and 5 mL of dry, degassed dichloromethane. After removal of the solvent, we obtained 40 mg (100%) of [**12**·Ag]$^+$[CF_3SO_3]$^-$ as a colorless powder, m.p. 281 °C (dec.). ^{1}H NMR (300 MHz, CD_2Cl_2): δ = 2.78 (br., s, 12 H, CH_2–N), 2.93 (t, ^3J = 5.8 Hz, 12 H, CH_2–Ar), 6.89 (br., s, 12 H, H_{ar}) ppm. ^{13}C NMR (75 MHz, CD_2Cl_2): δ = 31.1 (CH_2–Ar), 52.7 (CH_2–N), 126.5 (br., t-C_{ar}), 136.8 (q-C_{ar}) ppm. HRMS (FAB+): $^{12}C_{30}{}^1H_{36}{}^{109}Ag^{14}N_2$: calcd. 533.1926; found 533.1949; $^{12}C_{30}{}^1H_{36}{}^{107}Ag^{14}N_2$: calcd. 531.1930; found 531.1931. IR (KBr): $\tilde{\nu}$ = 2962 (m), 2907 (w), 2785 (w), 1512 (w), 1456 (m), 1380 (w), 1264 (s), 1223 (m), 1097 (m), 1034 (s), 802 (m), 640 (m) cm^{-1}.

(1,8-Diazabicyclo[6.6.6]eicosa-4,11,17-triyne)copper(I) Trifluoromethanesulfonate ([6·Cu]$^+$[CF_3SO_3]$^-$): Starting materials: **6** (30 mg, 0.1 mmol), $CuCF_3SO_3$·0.5C_6H_6 (30 mg, 0.1 mmol) and 5 mL of dry, degassed dichloromethane. After removal of the solvent and washing of the residue with dry toluene, we obtained 50 mg (95%) of [**6**·Cu]$^+$[CF_3SO_3]$^-$ as a colorless powder, m.p. 245 °C (dec.). ^{1}H NMR (300 MHz, CD_3OD): δ = 2.67 (s, 24 H, N–CH_2–CH_2–C≡) ppm. ^{13}C NMR (75 MHz, CD_3OD): δ = 19.0 (*C*H_2–C≡), 53.9 (CH_2–N), 81.2 (C≡C) ppm. HRMS (FAB+): $^{12}C_{18}{}^1H_{24}{}^{65}Cu^{14}N_2$: calcd. 333.1218; found 333.1239; $^{12}C_{18}{}^1H_{24}{}^{63}Cu^{14}N_2$: calcd. 331.1235; found 331.1241. IR (KBr): $\tilde{\nu}$ = 2964, 2922, 2870, 1457, 1264, 1225, 1158, 1106, 1031 cm^{-1}.

(1,8-Diazabicyclo[6.6.5]nonadeca-4,11,17-diyne)copper(I) Trifluoromethanesulfonate ([7·Cu]$^+$[CF_3SO_3]$^-$): Starting materials: **7** (15 mg, 0.06 mmol), $CuCF_3SO_3$·0.5C_6H_6 (16 mg, 0.06 mmol) and 5 mL of dry, degassed dichloromethane. After removal of the solvent, the residue was recrystallized from chloroform to yield 19 mg (62%) of [**7**·Cu]$^+$[CF_3SO_3]$^-$ as a colorless powder, m.p. 166 °C (dec.). ^{1}H NMR (300 MHz, $CDCl_3$): δ = 1.67–1.87 (m, 4 H, 2 CH_2), 1.92–1,97 (quint, ^3J = 7.0 Hz, 2 H, CH_2), 2.42–2.88 (m, 20 H, 10 CH_2) ppm. ^{13}C NMR (75 MHz, $CDCl_3$): δ = 20.4 (*C*H_2–C≡), 20.3 (*C*H_2), 25.7 (*C*H_2), 53.5 (*C*H_2–N), 55.1 (*C*H_2–N), 82.8 (C≡C) ppm. IR (KBr): $\tilde{\nu}$ = 3103, 2927, 1630, 1458, 1261, 1158, 1031 cm^{-1}. HRMS (FAB+): $C_{17}H_{26}{}^{63}CuN_2$: calcd. 321.1392; found 321.1392; $C_{17}H_{26}{}^{65}CuN_2$: calcd. 323.1401; found 323.1397.

(1,8-Diazabicyclo[6.6.6]eicosa-4,11-diyne)copper(I) Trifluoromethanesulfonate ([8·Cu$^+$]$^+$[CF_3SO_3]$^-$): Starting materials: **8** (15 mg, 0.06 mmol), $CuCF_3SO_3$·0.5C_6H_6 (16 mg, 0.06 mmol) and 5 mL of dry, degassed dichloromethane. After removal of the solvent and washing of the residue with dry toluene, we obtained 17 mg (64%) of [**8**·Cu]$^+$[CF_3SO_3]$^-$ as a colorless powder. ^{1}H NMR (300 MHz, CD_2Cl_2): δ = 1.67–1.83 (m, 8 H, CH_2), 2.61–2.77 (m, 20 H, CH_2–N, CH_2–C≡) ppm. ^{13}C NMR (75 MHz, CD_2Cl_2): δ = 18.3 (*C*H_2–C≡), 22.4 (CH_2), 23.9 (CH_2), 51.9 (N–*C*H_2–CH_2–CH_2), 54.5 (N–*C*H_2–CH_2–C≡), 81.0 (C≡C) ppm. HRMS (FAB+): $^{12}C_{18}{}^1H_{28}{}^{65}Cu^{14}N_2$: calcd. 337.1530; found 337.1517; $^{12}C_{18}{}^1H_{28}{}^{63}Cu^{14}N_2$: calcd. 335.1548; found 335.1510.

(1,10-Diazabicyclo[8.6.6]docosa-5,13,19-triyne)copper(I) Trifluoromethanesulfonate ([9·Cu]$^+$[CF_3SO_3]$^-$): Starting materials: **9** (19 mg, 0.06 mmol), $CuCF_3SO_3$·0.5C_6H_6 (23 mg, 0.09 mmol) and 10 mL of dry, degassed dichloromethane. After removal of the solvent and washing of the residue with dry toluene, we obtained 22 mg (68%) of [**9**·Cu]$^+$[CF_3SO_3]$^-$ as a colorless powder, m.p. 149 °C (dec.). ^{1}H NMR (300 MHz, CD_2Cl_2): δ = 1.87 (pseudo-quint, 4 H, CH_2–CH_2–CH_2), 2.51 (m, 4 H, CH_2–C≡), 2.66 (m, 16 H, CH_2–N, CH_2–C≡), 2.70 (t, ^3J = 6.4 Hz, 4 H, CH_2–N) ppm. ^{13}C NMR (75 MHz, CD_2Cl_2): δ = 17.2 (2 C, *C*H_2–C≡), 20.0 (4 C, *C*H_2–C≡), 23.9 (CH_2–*C*H_2–CH_2), 53.3 (4 C, CH_2–N), 53.7 (2 C, CH_2–N), 80.5 (4 C, C≡C), 81.2 (2 C, C≡C) ppm. HRMS (FAB+): $^{12}C_{20}{}^1H_{28}{}^{65}Cu^{14}N_2$: calcd. 361.1531; found 361.1505; $^{12}C_{20}{}^1H_{28}{}^{63}Cu^{14}N_2$: calcd. 359.1549; found 359.1501. IR (KBr): $\tilde{\nu}$ = 2921 (m), 1455 (m), 1277 (vs), 1146 (s), 1031 (s), 803 (m), 638 (s), 518 (m) cm^{-1}.

{17-(1,4)Benzena-1,8-diazabicyclo[6.6.5]nonadecaphane-4,11-diyne}copper(I) Trifluoromethanesulfonate ([10·Cu]$^+$[CF_3SO_3]$^-$): Starting materials: **10** (15 mg, 0.05 mmol), $CuCF_3SO_3$·0.5C_6H_6 (13 mg, 0.05 mmol), 5 mL of dry, degassed dichloromethane. After removal of the solvent and washing of the residue with dry toluene, we obtained 15 mg (60%) of [**10**·Cu]$^+$[CF_3SO_3]$^-$ as a colorless powder, m.p. 245 °C (dec.). ^{1}H NMR (300 MHz, CD_2Cl_2): δ = 2.42–2.74 (m, 16 H, N–CH_2–CH_2–C≡), 2.82–2.98 (m, 8 H, N–CH_2–CH_2–Ar), 7.26 (s, 4 H, H_{ar}) ppm. ^{13}C NMR (75 MHz, CD_2Cl_2): δ = 20.9 (*C*H_2–C≡), 31.8 (CH_2–Ar), 51.9 (N–*C*H_2–CH_2–C≡), 54.9 (CH_2–N), 82.8 (C≡C), 128.6 (t-C_{ar}), 136.3 (q-C_{ar}) ppm. HRMS (FAB+): $^{12}C_{22}{}^1H_{28}{}^{65}Cu^{14}N_2$: calcd. 385.1531; found 385.1550; $^{12}C_{22}{}^1H_{28}{}^{63}Cu^{14}N_2$: calcd. 383.1548; found 383.1542.

{11,16-(1,4)Dibenzena-1,8-diazabicyclo[6.5.5]octadecaphane-4-yne}copper(I) Trifluoromethanesulfonate ([11·Cu]$^+$[CF_3SO_3]$^-$): Starting materials: **11** (15 mg, 0.04 mmol), $CuCF_3SO_3$·0.5C_6H_6 (13 mg, 0.05 mmol) and 5 mL of dry, degassed CH_2Cl_2. After removal of the solvent and washing of the residue with dry toluene, we obtained 18 mg (78%) of [**11**·Cu]$^+$[CF_3SO_3]$^-$ as a colorless powder, m.p. 282 °C (dec.). ^{1}H NMR (300 MHz, CD_2Cl_2): δ = 2.39 (s, 8 H, N–*C*H_2–CH_2–C≡), 270–3.13 (m, 16 H, N–*C*H_2–CH_2–Ar), 7.16 (s, 4 H, H_{ar}), 7.19 (s, 4 H, H_{ar}) ppm. ^{13}C NMR (75 MHz, CD_2Cl_2): δ = 20.4 (*C*H_2–C≡), 31.8 (CH_2–Ar), 50.1 (N–*C*H_2–CH_2–C≡), 53.8 (CH_2–N), 82.4 (C≡C), 124.8 (t-C_{ar}), 129.9 (t-C_{ar}), 136.3 (q-C_{ar}) ppm. HRMS (FAB+): $^{12}C_{26}{}^1H_{32}{}^{65}Cu^{14}N_2$: calcd. 437.1843; found 437.1842; $^{12}C_{26}{}^1H_{32}{}^{63}Cu^{14}N_2$: calcd. 435.1861; found 435.1839.

{4,10,15-(1,4)Tribenzena-1,7-diazabicyclo[5.5.5]heptadecaphane}-copper(I) Trifluoromethanesulfonate ([12·Cu]$^+$[CF_3SO_3]$^-$): Starting materials: **12** (20 mg, 0.05 mmol), $CuCF_3SO_3$·0.5C_6H_6 (13 mg, 0.05 mmol) and 5 mL of dry, degassed dichloromethane. After removal of the solvent and washing of the residue with dry toluene, we obtained 32 mg (98%) of [**12**·Cu]$^+$[CF_3SO_3]$^-$ as a colorless powder, m.p. 298 °C (dec.). ^{1}H NMR (500 MHz, CD_2Cl_2): δ = 2.95 (br. s, 24 H, CH_2), 6.68 (br. s, 12 H, H_{ar}) ppm. ^{13}C NMR (125 MHz, CD_2Cl_2): δ = 30.6 (CH_2–Ar), 52.2 (CH_2–N), 124.7 (br., t-C_{ar}), 137.5 (q-C_{ar}) ppm. HRMS (FAB+): $^{12}C_{30}{}^1H_{36}{}^{65}Cu^{14}N_2$: calcd. 489.2156; found 489.2172; $^{12}C_{30}{}^1H_{36}{}^{63}Cu^{14}N_2$: calcd. 487.2175; found 487.2186. IR(KBr): $\tilde{\nu}$ = 2962 (m), 2924 (w), 2856 (m), 2783 (m), 1513 (m), 1460 (m), 1268 (vs), 1222 (s), 1145 (s), 1096 (s), 1032 (s), 800 (s), 638 (m) cm^{-1}.

Quantum Chemical Calculations: The geometrical parameters of **11** (Table 2) were derived from density functional theory (DFT)[17] calculations using Becke's three-parameter hybrid functional[30] combined with the Lee–Yang–Parr[31] correlation functional (abbreviated B3LYP). The calculations were performed with the GAUSSIAN98 program package[32] using the 3-21G basis set.[33] The $\Delta G^{\neq}$ values listed in Table 1 for **10**–**12** were derived from the semiemperical AM1 procedure[15] adopting either the experimental determined geometrical parameters (**10**, **12**) or the calculated values (**11**).

X-ray Structure Analyses: The reflexions were mostly collected with a Bruker Smart CCD diffractometer (**9**: Nonius CAD 4) with Mo-K_α radiation at 200 K {**9**, [**10**·Cu](CF_3SO_3), [**12**·Ag](CF_3SO_3), and [**12**·Cu](CF_3SO_3) at room temperature}. Sets of 0.3° ω-scans with CCD area detector were taken, covering a whole sphere in reciprocal space in the majority of cases {**9**: asymmetric unit with ω-2θ

scans and point detector; [**7**·Ag](CF_3SO_3): hemisphere}. Intensities were corrected for Lorentz and polarization effects, and an empirical absorption correction was applied using SADABS[34] based on the Laue symmetry of the reciprocal space (except for **9**). Structures were solved by direct methods and refined against F^2 with a full-matrix least-squares algorithm using the SHELXTL-PLUS (5.10) software package[35]. Hydrogen atoms were treated using appropriate riding models in most cases, except for the hydrogen atoms of the free ligands **9** and **10** and the protons of [**6**·H]$^+$ and [**12**·H]$^+$, which were refined isotropically. In many cases the solid-state structure was found to be disordered in a common way: Without affecting the outer shape of the complexes or the coordination properties significantly one or both $N(CH_2–)_3$ units can rotate by about 60° around the local C_3 axis. This type of disorder is realised in [**6**·H]$^+$, [**12**·H]$^+$, [**7**·Cu]$^+$, [**8**·Ag]$^+$, [**9**·Ag]$^+$, [**10**·Ag]$^+$, [**12**·Ag]$^+$, and [**12**·Cu]$^+$ with occupancies for the minor component from 10% up to 50%. In the case of [**7**·Cu]$^+$ and [**8**·Ag]$^+$ also some atoms of the bridging alkyl chains are affected by this disorder, in [**12**·Cu]$^+$ we find tilting aryl rings correlated with this disorder. Some of the complexes tend to undergo phase transitions on cooling, which assumably is related to "freezing out" this type of disorder. In [**7**·Cu]$^+$ the Cu atom is partially replaced by a proton (44%), in [**9**·Cu]$^+$, [**10**·Cu]$^+$, and [**12**·Ag]$^+$ the metal ion occupies two different positions inside the prismand, in the former complex unsymmetrically 84:16, in the other two complexes symmetry-imposed with equal occupation. The structure of [**10**·Cu]$^+$ is of very poor quality. In addition to the mentioned disorder of the Cu atom there is disorder of a methylene bridge and the triflate anion resides on a fourfold axis, which of course causes severe disorder. In [**12**·Ag]$^+$ the triflate anion is located on a mirror plane perpendicular to the C–S axis which leads to disorder probably correlated to the two different Ag positions in this complex. CCDC-298184 to -298196 and -145166 contain the supplementary crystallographic data for this paper. These data can be obtained free of charge from The Cambridge Crystallographic Data Centre via www.ccdc.cam.ac.uk/data_request/cif.

9: Colorless crystal (plate), dimensions 0.50 × 0.45 × 0.15 mm, crystal system monoclinic, space group $P2_1/n$, Z = 4, a = 7.638(2) Å, b = 7.948(2) Å, c = 29.051(7) Å, β = 92.36(2)°, V = 1762.1(8) Å^3, ρ = 1.117 g/cm^3, T = 293(2) K, Θ_{max} = 27.99°, 4556 reflections measured, 4246 unique (R_{int} = 0.0443), 2309 observed [$I > 2\sigma(I)$], μ = 0.06 mm^{-1}, 311 parameters refined, goodness of fit 1.01 for observed reflections, final residual values $R(F)$ = 0.048, $wR(F^2)$ = 0.119 for observed reflections, residual electron density –0.21 to 0.30 e·Å^{-3}, CCDC-298184.

10: Colorless crystal (polyhedron), dimensions 0.36 × 0.26 × 0.22 mm, crystal system monoclinic, space group $P2_1/n$, Z = 4, a = 10.4021(2) Å, b = 14.4056(2) Å, c = 13.0903(1) Å, β = 106.864(1)°, V = 1877.21(5) Å^3, ρ = 1.134 g/cm^3, T = 200(2) K, Θ_{max} = 27.44°, 18863 reflections measured, 4284 unique (R_{int} = 0.0355), 3057 observed [$I > 2\sigma(I)$], μ = 0.07 mm^{-1}, T_{min} = 0.70, T_{max} = 0.93, 329 parameters refined, goodness of fit 1.03 for observed reflections, final residual values $R(F)$ = 0.040, $wR(F^2)$ = 0.094 for observed reflections, residual electron density –0.18 to 0.15 e·Å^{-3}, CCDC-298185.

[6·H]$^+$(BF_4)$^–$: Colorless crystal (polyhedron), dimensions 0.77 × 0.18 × 0.07 mm, crystal system triclinic, space group $P\bar{1}$, Z = 2, a = 8.2076(8) Å, b = 9.9446(9) Å, c = 12.1243(11) Å, α = 73.0150(10)°, β = 81.3800(10)°, γ = 85.5350(10)°, V = 935.14(15) Å^3, ρ = 1.265 g/cm^3, T = 200(2) K, Θ_{max} = 25.40°, 7042 reflections measured, 3124 unique (R_{int} = 0.0216), 2243 observed [$I > 2\sigma(I)$], μ = 0.10 mm^{-1}, 303 parameters refined, goodness of fit 1.02 for observed reflections, final residual values $R(F)$ = 0.054, $wR(F^2)$ = 0.140 for observed reflections, residual electron density –0.24 to 0.49 e·Å^{-3}, CCDC-298186.

[12·H]$^+$(CF_3COO)$^–$: Colorless crystal (polyhedron), dimensions 0.30 × 0.20 × 0.18 mm, crystal system monoclinic, space group $P2_1$, Z = 2, a = 8.5818(4) Å, b = 11.8542(5) Å, c = 13.5266(6) Å, β = 92.5390(10)°, V = 1374.72(11) Å^3, ρ = 1.301 g/cm^3, T = 200(2) K, Θ_{max} = 27.50°, 14267 reflections measured, 6283 unique (R_{int} = 0.0491), 3765 observed [$I > 2\sigma(I)$], μ = 0.09 mm^{-1}, T_{min} = 0.79, T_{max} = 0.98, 397 parameters refined, Flack absolute structure parameter 1.7(13), goodness of fit 1.01 for observed reflections, final residual values $R(F)$ = 0.060, $wR(F^2)$ = 0.117 for observed reflections, residual electron density –0.23 to 0.22 e·Å^{-3}, CCDC-298187.

[7·Ag]$^+$(CF_3SO_3)$^–$: Colorless crystal (polyhedron), dimensions 0.34 × 0.10 × 0.02 mm, crystal system orthorhombic, space group $Pbca$, Z = 8, a = 9.0306(3) Å, b = 16.8259(5) Å, c = 26.1579(4) Å, V = 3974.64(19) Å^3, ρ = 1.722 g/cm^3, T = 200(2) K, Θ_{max} = 27.48°, 27623 reflections measured, 4550 unique (R_{int} = 0.0868), 2970 observed [$I > 2\sigma(I)$], μ = 1.17 mm^{-1}, T_{min} = 0.69, T_{max} = 0.98, 253 parameters refined, goodness of fit 1.00 for observed reflections, final residual values $R(F)$ = 0.035, $wR(F^2)$ = 0.061 for observed reflections, residual electron density –0.63 to 0.40 e·Å^{-3}, CCDC-298188.

[7·Cu]$^+$(CF_3SO_3)$^–$: Colorless crystal (polyhedron), dimensions 0.34 × 0.14 × 0.04 mm, crystal system monoclinic, space group $P2_1/n$, Z = 4, a = 11.6825(3) Å, b = 12.9405(2) Å, c = 14.1559(3) Å, β = 113.3980(10)°, V = 1964.07(7) Å^3, ρ = 1.593 g/cm^3, T = 200(2) K, Θ_{max} = 24.74°, 16154 reflections measured, 3358 unique (R_{int} = 0.0705), 2579 observed [$I > 2\sigma(I)$], μ = 1.27 mm^{-1}, T_{min} = 0.67, T_{max} = 0.95, 310 parameters refined, goodness of fit 1.33 for observed reflections, final residual values $R(F)$ = 0.087, $wR(F^2)$ = 0.195 for observed reflections, residual electron density –0.70 to 0.47 e·Å^{-3}, CCDC-298189.

[8·Ag]$^+$(CF_3SO_3)$^–$: Colorless crystal (polyhedron), dimensions 0.28 × 0.17 × 0.14 mm, crystal system monoclinic, space group $P2_1/n$, Z = 4, a = 12.0922(3) Å, b = 13.0157(3) Å, c = 14.1538(3) Å, β = 109.2330(10)°, V = 2103.31(8) Å^3, ρ = 1.672 g/cm^3, T = 200(2) K, Θ_{max} = 27.51°, 21196 reflections measured, 4822 unique (R_{int} = 0.0346), 4002 observed [$I > 2\sigma(I)$], μ = 1.11 mm^{-1}, T_{min} = 0.80, T_{max} = 0.88, 283 parameters refined, goodness of fit 1.06 for observed reflections, final residual values $R(F)$ = 0.027, $wR(F^2)$ = 0.064 for observed reflections, residual electron density –0.57 to 0.67 e·Å^{-3}, CCDC-298190.

[9·Ag]$^+$(CF_3SO_3)$^–$: Colorless crystal (polyhedron), dimensions 0.54 × 0.22 × 0.08 mm, crystal system monoclinic, space group $P2_1/c$, Z = 4, a = 12.7551(8) Å, b = 8.1937(5) Å, c = 22.1464(14) Å, β = 103.3630(10)°, V = 2251.9(2) Å^3, ρ = 1.632 g/cm^3, T = 200(2) K, Θ_{max} = 25.59°, 16322 reflections measured, 3943 unique (R_{int} = 0.0209), 3517 observed [$I > 2\sigma(I)$], μ = 1.04 mm^{-1}, T_{min} = 0.73, T_{max} = 0.94, 293 parameters refined, goodness of fit 1.09 for observed reflections, final residual values $R(F)$ = 0.025, $wR(F^2)$ = 0.063 for observed reflections, residual electron density –1.10 to 0.43 e·Å^{-3}, CCDC-298191.

[9·Cu]$^+$(CF_3SO_3)$^–$: Colorless crystal (polyhedron), dimensions 0.32 × 0.14 × 0.12 mm, crystal system monoclinic, space group $P2_1/c$, Z = 4, a = 7.3972(2) Å, b = 19.1054(6) Å, c = 15.2348(5) Å, β = 93.3680(10)°, V = 2149.36(11) Å^3, ρ = 1.573 g/cm^3, T = 200(2) K, Θ_{max} = 27.49°, 22026 reflections measured, 4933 unique (R_{int} = 0.0649), 3265 observed [$I > 2\sigma(I)$], μ = 1.16 mm^{-1}, T_{min} = 0.71, T_{max} = 0.89, 285 parameters refined, goodness of fit 1.00 for observed reflections, final residual values $R(F)$ = 0.041, $wR(F^2)$ =

0.083 for observed reflections, residual electron density –0.60 to 0.34 e·Å^{-3}, CCDC-298192.

[10·Ag]$^+$(CF$_3$SO$_3$)$^-$: Colorless crystal (polyhedron), dimensions 0.45 × 0.17 × 0.06 mm, crystal system monoclinic, space group $P2_1/c$, Z = 4, a = 7.5177(2) Å, b = 14.7642(4) Å, c = 20.6346(5) Å, β = 91.5710(10)°, V = 2289.43(10) Å^3, ρ = 1.675 g/cm^3, T = 200(2) K, Θ_{max} = 27.48°, 23199 reflections measured, 5255 unique (R_{int} = 0.0365), 4350 observed [$I > 2\sigma(I)$], μ = 1.02 mm^{-1}, T_{min} = 0.77, T_{max} = 0.95, 326 parameters refined, goodness of fit 1.04 for observed reflections, final residual values $R(F)$ = 0.027, $wR(F^2)$ = 0.060 for observed reflections, residual electron density –0.65 to 0.41 e·Å^{-3}, CCDC-298193.

[10·Cu]$^+$(CF$_3$SO$_3$)$^-$: Colorless crystal (polyhedron), dimensions 0.50 × 0.20 × 0.08 mm, crystal system tetragonal, space group $I4cm$, Z = 4, a = b = 12.6877(5) Å, c = 14.5975(9) Å, V = 2349.9(2) Å^3, ρ = 1.507 g/cm^3, T = 298(2) K, Θ_{max} = 27.49°, 4872 reflections measured, 1337 unique (R_{int} = 0.0772), 515 observed [$I > 2\sigma(I)$], μ = 1.07 mm^{-1}, T_{min} = 0.69, T_{max} = 0.93, 86 parameters refined, Flack absolute structure parameter 0.13(10), goodness of fit 1.75 for observed reflections, final residual values $R(F)$ = 0.143, $wR(F^2)$ = 0.323 for observed reflections, residual electron density –0.54 to 0.62 e·Å^{-3}, CCDC-298194.

[11·Ag]$^+$(CF$_3$SO$_3$)$^-$: Colorless crystal (polyhedron), dimensions 0.40 × 0.11 × 0.10 mm, crystal system monoclinic, space group $P2_1/n$, Z = 4, a = 8.6371(1) Å, b = 11.8248(2) Å, c = 25.6656(3) Å, β = 90.76°, V = 2621.05(6) Å^3, ρ = 1.595 g/cm^3, T = 200(2) K, Θ_{max} = 27.45°, 26292 reflections measured, 5975 unique (R_{int} = 0.0446), 4452 observed [$I > 2\sigma(I)$], μ = 0.90 mm^{-1}, T_{min} = 0.67, T_{max} = 0.82, 334 parameters refined, goodness of fit 1.02 for observed reflections, final residual values $R(F)$ = 0.032, $wR(F^2)$ = 0.071 for observed reflections, residual electron density –0.41 to 1.02 e·Å^{-3}, CCDC-298195.

[12·Ag]$^+$(CF$_3$SO$_3$)$^-$: Colorless crystal (polyhedron), dimensions 0.42 × 0.34 × 0.06 mm, crystal system hexagonal, space group $P6_3/m$, Z = 2, a = b = 9.2053(4) Å, c = 19.8081(11) Å, γ = 120°, V = 1453.61(12) Å^3, ρ = 1.557 g/cm^3, T = 298(2) K, Θ_{max} = 27.52°, 14903 reflections measured, 1150 unique (R_{int} = 0.0565), 794 observed [$I > 2\sigma(I)$], μ = 0.82 mm^{-1}, T_{min} = 0.77, T_{max} = 0.97, 81 parameters refined, goodness of fit 1.02 for observed reflections, final residual values $R(F)$ = 0.037, $wR(F^2)$ = 0.088 for observed reflections, residual electron density –0.25 to 0.17 e·Å^{-3}, CCDC-145166.

[12·Cu]$^+$(CF$_3$SO$_3$)$^-$: Colorless crystal (polyhedron), dimensions 0.17 × 0.10 × 0.08 mm, crystal system trigonal, space group $P31c$, Z = 2, a = b = 9.1182(1) Å, c = 20.3381(2) Å, γ = 120°, V = 1464.40(3) Å^3, ρ = 1.445 g/cm^3, T = 298(2) K, Θ_{max} = 27.42°, 14261 reflections measured, 2245 unique (R_{int} = 0.1895), 1515 observed [$I > 2\sigma(I)$], μ = 0.87 mm^{-1}, T_{min} = 0.74, T_{max} = 0.94, 191 parameters refined, Flack absolute structure parameter 0.52(4), goodness of fit 1.07 for observed reflections, final residual values $R(F)$ = 0.074, $wR(F^2)$ = 0.162 for observed reflections, residual electron density –0.85 to 0.54 e·Å^{-3}, CCDC-298196.

Acknowledgments

We are grateful to the Deutsche Forschungsgemeinschaft for financial support. S. B. thanks the Alexander von Humboldt Foundation for a stipendium.

[1] a) H. E. Simmons, C. H. Park, R. T. Uyeda, M. F. Habibi, *Trans. N. Y. Acad. Sci. Ser. II* **1970**, *32*, 521–534; b) H. E. Simmons, C. H. Park, *J. Am. Chem. Soc.* **1968**, *90*, 2428–2429; c) C. H. Park, H. E. Simmons, *J. Am. Chem. Soc.* **1968**, *90*, 2429–2431.
[2] a) R. W. Alder, S. P. East, *Chem. Rev.* **1996**, *96*, 2097–2112; b) R. W. Alder, *Chem. Rev.* **1989**, *89*, 1215–1223; R. W. Alder, *Tetrahedron* **1990**, *46*, 683–713; R. W. Alder, *Acc. Chem. Res.* **1983**, *16*, 321–327.
[3] a) R. W. Alder, R. F. Moss, R. B. Sessions, *J. Chem. Soc., Chem. Commun.* **1983**, 997–998; b) R. W. Alder, A. G. Orpen, R. B. Sessions, *J. Chem. Soc., Chem. Commun.* **1983**, 999–1000.
[4] B. Pool, S. Balalaie, A. Kunze, G. Schilling, P. Bischof, R. Gleiter, *Eur. J. Org. Chem.* **2004**, 2812–2817.
[5] J. Cheney, J.-M. Lehn, *J. Chem. Soc., Chem. Commun.* **1972**, 487–489.
[6] a) A. Kunze, F. Rominger, R. Gleiter, *Eur. J. Inorg. Chem.* **2006**, 621–627; b) R. Koschabek, F. Rominger, R. Gleiter, *Eur. J. Inorg. Chem.* **2006**, 609–620.
[7] J.-L. Pierre, P. Baret, P. Chautemps, M. Armand, *J. Am. Chem. Soc.* **1981**, *103*, 2986–2988.
[8] a) V. Wolfart, R. Gleiter, H. Irngartinger, T. Oeser, C. Krieger, *Eur. J. Org. Chem.* **1998**, 2803–2809; b) V. Wolfart, R. Gleiter, C. Krüger, H. Pritzkow, *Tetrahedron Lett.* **1998**, *39*, 513–516.
[9] A. Kunze, S. Bethke, R. Gleiter, F. Rominger, *Org. Lett.* **2000**, *2*, 609–612.
[10] M. Brudermüller, H. Musso, A. Wagner, *Chem. Ber.* **1988**, *121*, 2239–2244.
[11] T. v. Hirschheydt, V. Wolfart, R. Gleiter, H. Irngartinger, T. Oeser, F. Rominger, F. Eisenträger, *J. Chem. Soc., Perkin Trans. 2* **2000**, 175–183.
[12] a) R. Gleiter, R. Merger, in: *Modern Acetylene Chemistry* (Ed.: P. J. Stang, F. Diederich), VCH, Weinheim, **1995**, p. 285–319; b) M. Hesse, H. Meier, B. Zeeh, *Spectroscopic Methods in Organic Chemistry*, Georg Thieme Verlag, Stuttgart, **1997**.
[13] *UV-Atlas of Organic Compounds*, Verlag Chemie, Weinheim and Butterworths, London, **1967**, vol. 3.
[14] H. Kessler, *Angew. Chem.* **1970**, *82*, 237–253; H. Friebolin, *Basic One- and Two-Dimensional NMR Spectroscopy*, Wiley-VCH, Weinheim, **1999**.
[15] M. J. S. Dewar, E. G. Zoebisch, E. F. Healy, J. J. P. Stewart, *J. Am. Chem. Soc.* **1985**, *107*, 3902–3909.
[16] a) R. G. Parr, W. Yang, *Density Functional Theory of Atoms and Molecules*, Oxford University Press, Oxford, U. K., **1989**.
[17] W. Koch, M. C. Holthausen, *A Chemist's Guide to Density Functional Theory*, Wiley-VCH, Weinheim, **2001**.
[18] A. Kunze, R. Gleiter, F. Rominger, *Chem. Commun.* **1999**, 171–172.
[19] a) U. Zachwieja, H. Jacobs, *Z. Kristallogr.* **1992**, *201*, 207–212; b) R. Gleiter, T. v. Hirschheydt, F. Rominger, *Eur. J. Inorg. Chem.* **2000**, 2127–2130.
[20] F. A. Allen, *Acta Crystallogr., Sect. B* **2002**, *58*, 380–388.
[21] a) J. D. Ferrara, A. Djebli, C. Tessier Youngs, W. J. Youngs, *J. Am. Chem. Soc.* **1988**, *110*, 647–649; b) R. Gleiter, M. Karcher, D. Kratz, M. L. Ziegler, B. Nuber, *Chem. Ber.* **1990**, *123*, 1461–1468; c) H. Maier, Y. Dai, *Tetrahedron Lett.* **1993**, *34*, 5277–5280; d) T. Nishinaga, T. Kawamura, K. Komatsu, *Chem. Commun.* **1998**, 2263–2264; e) P. Schulte, U. Behrens, *J. Organomet. Chem.* **1998**, *563*, 235–249; f) K. M. Chi, C. T. Lin, S. M. Peng, G.-H. Lee, *Organometallics* **1996**, *15*, 2660–2663.
[22] G. Gröger, U. Behrens, F. Olbrich, *Organometallics* **2000**, *19*, 3354–3360 and references cited therein; D. L. Reger, M. F. Huff, T. A. Wolfe, R. D. Adams, *Organometallics* **1989**, *8*, 848–850.
[23] L. Pauling, *The Nature of the Chemical Bond*, 3rd ed., Cornell University Press, Ithaca, N. Y., **1960**.
[24] H. C. Kang, A. W. Hanson, B. Eaton, V. Boekelheide, *J. Am. Chem. Soc.* **1985**, *107*, 1979–1985.
[25] J. Groß, G. Harder, A. Siepen, J. Harren, F. Vögtle, H. Stephan, K. Gloe, B. Ahlers, K. Cammann, K. Rissanen, *Chem. Eur. J.* **1996**, *2*, 1585–1595.

[26] J. Gross, G. Harder, F. Vögtle, H. Stephan, K. Gloe, *Angew. Chem.* **1995**, *107*, 523–526; *Angew. Chem. Int. Ed. Engl.* **1995**, *34*, 481–484.
[27] R. W. Turner, E. L. Amma, *J. Am. Chem. Soc.* **1966**, *88*, 1877–1882.
[28] J. T. Longone, S. H. Küsefoglu, J. A. Gladysz, *J. Org. Chem.* **1977**, *42*, 2787–2788.
[29] P. Ruggli, B. Prijs, *Helv. Chim. Acta* **1945**, *28*, 674–690.
[30] a) A. D. Becke, *J. Chem. Phys.* **1992**, *96*, 2155–2160; b) A. D. Becke, *J. Chem. Phys.* **1993**, *98*, 5648–5652.
[31] C. Lee, W. Yang, R. G. Parr, *Phys. Rev. B* **1988**, *37*, 785–789.
[32] M. J. Frisch, G. W. Trucks, H. B. Schlegel, G. E. Scuseria, M. A. Robb, J. R. Cheeseman, V. G. Zakrzewski, J. A. Montgomery Jr, R. E. Stratmann, J. C. Burant, S. Dapprich, J. M. Millam, A. D. Daniels, K. N. Kudin, M. C. Strain, O. Farkas, J. Tomasi, V. Barone, M. Cossi, R. Cammi, B. Mennucci, C. Pomelli, C. Adamo, S. Clifford, J. Ochterski, G. A Petersson, P. Y. Ayala, Q. Cui, K. Morokuma, D. K. Malick, A. D. Rabuck, K.Raghavachari, J. B. Foresman, J. Cioslowski, J. V. Ortiz, B. B. Stefanov, G. Liu, A. Liashenko, P. Piskorz, I. Komaromi, R. Gomperts, R. L.Martin, D. J: Fox, T. Keith, M. A. Al-Laham, C. Y. Peng, A. Nanayakkara, C. Gonzalez, M. Challacombe, P. M. W. Gill, B. Johnson, W. Chen, M. W. Wong, J. L. Andres, C. Gonzales, M. Head-Gordon, E. S. Replogle, J. A. Pople, *Gaussian 98*, Revision A.5, Gaussian, Inc., Pittsburgh, PA, **1998**.
[33] K. Krishnan, J. S. Binkley, R. Seeger, J. A. Pople, *Chem. Phys.* **1980**, *72*, 650–654.
[34] G. M. Sheldrick, Bruker Analytical X-ray-Division, Madison, Wisconsin **2001**.
[35] G. M. Sheldrick, Bruker Analytical X-ray-Division, Madison, Wisconsin **1997**.

Received: February 6, 2006
Published Online: May 2, 2006

